



City Research Online

City St George's, University of London

Citation: Kanthasamy, E., Thirunavukkarasu, K., Poologanathan, K., Gunalan, S., Gatheeshgar, P., Tsavdaridis, K. D. & Corradi, M. (2023). Flexural Behaviour and Design Rules for SupaCee Sections with Web Openings. *Journal of Building Engineering*, 63(Part A), 105539. doi: 10.1016/j.jobe.2022.105539

This is the accepted version of the paper.

This version of the publication may differ from the final published version. To cite this item please consult the publisher's version.

Permanent repository link: <https://openaccess.city.ac.uk/id/eprint/29215/>

Link to published version: <https://doi.org/10.1016/j.jobe.2022.105539>

Copyright and Reuse: Copyright and Moral Rights remain with the author(s) and/or copyright holders. Copies of full items can be used for personal research or study, educational, or not-for-profit purposes without prior permission or charge, unless otherwise indicated, provided that the authors, title and full bibliographic details are credited, a hyperlink and/or URL is given for the original metadata page and the content is not changed in any way. For full details of reuse please refer to [City Research Online policy](#).

1 **Flexural behaviour and design rules for SupaCee**
2 **sections with web openings**

3
4 **Kajaharan Thirunavukkarasu**

5 Institute of Technology, University of Moratuwa, Homagama, Sri Lanka

6 **Elilarasi Kanthasamy**

7 Faculty of Engineering and Environment, Northumbria University, Newcastle upon Tyne, UK

8 **Keerthan Poologanathan**

9 Faculty of Engineering and Environment, Northumbria University, Newcastle upon Tyne, UK

10 **Shanmuganathan Gunalan**

11 School of Engineering and Built Environment, Griffith University, Queensland, Australia

12 **Perampalam Gatheeshgar**

13 School of Computing, Engineering and Digital Technologies, Teesside University, UK

14 **Konstantinos Daniel Tsavdaridis**

15 School of Mathematics, Computer Science and Engineering, City, University of London, UK

16 **Marco Corradi**

17 Faculty of Engineering and Environment, Northumbria University, Newcastle upon Tyne, UK

18 **Abstract:**

19 Cold-Formed Steel (CFS) has been used to a great extent due to the industry uptake given its
20 merits with the key being its high strength-to-weight ratio. Besides, innovative section profiles
21 are constantly introduced to uplift the structural applicability of CFS sections. SupaCee section
22 is a novel section with enhanced structural performance due to its sectional attributes such as
23 longitudinal web stiffeners and return lips. However, the necessity of web openings (holes) to
24 provide service integrations is not considered adequately so far in previous studies with
25 SupaCee sections. Hence, this study reports a comprehensive assessment on flexural
26 performance of SupaCee sections with web openings. Accordingly, numerical analysis was
27 carried out which followed by the validation of the elaborated Finite Element (FE) model and
28 the development of parametric studies considering key parameters such as depth, thickness,
29 yield strength, web opening ratio and hole spacing. Results from the numerical studies are
30 discussed and compared with existing design standards. New design provisions are proposed
31 to predict the flexural capacity of SupaCee sections with web openings. Moreover, FE model
32 of Lipped Channel Beam (LCB) was developed and analysed with similar parameters of
33 SupaCee sections. The comparison of LCB and SupaCee sections with and without web
34 openings are reported and based on the flexural capacity comparisons; recommendations are
35 stated to replace conventional CFS sections by SupaCee sections.

36 *Keywords: Cold-formed steel; SupaCee section; Flexural performance; Web opening; Finite*
37 *element modelling*

Nomenclature

d	Section depth	d_{wh}	Diameter of the hole
E	Modulus of elasticity	d_l	Clear web height
t	Thickness of the section	M_{ne}	Nominal member flexural strength for lateral torsional buckling
M	Ultimate bending capacity	M_{crl}	Critical elastic local buckling moment
f_y	Yield strength	λ_l	Non-dimensional slenderness value.
q_s	Reduction factor	M_{nd}	Nominal member moment capacity for distortional buckling
S	Hole spacing	M_y	Member yield moment
M_{nl}	Nominal member moment capacity at local buckling	M_{crg}	Critical elastic distortional buckling moment
M_p	Plastic moment	M_{ny}	Inelastic moment for extended slenderness limit;
C_{yd}	Distortional yield strain multiplier	C_{yl}	Local yield strain multiplier
M_{crlg}	Critical elastic local buckling moment at gross cross-section	M_{crlh}	critical local buckling moment of compressed section above the web opening
M_{crg}	Critical elastic distortional buckling moment of gross cross-section	M_{crgn}	Critical elastic distortional buckling moment at a web opening
I_x	Second moment of area		

38 **1 Introduction**

39 Cold-Formed Steel (CFS) sections are being used as primary and secondary load-bearing
40 members for over 100 years but have now been introduced into new areas of construction
41 including modular construction [1] due to their merits and efficiencies such as light weight,
42 high strength-to-weight ratio and flexibility. Meanwhile, highly optimised cross-section
43 profiles of CFS sections have been emerged to improve their structural performance. Fig.1
44 shows the innovative cross-section profiles which were introduced in the CFS industry across
45 various countries such as Australia, the United Kingdom and New Zealand. Subsequently,
46 SupaCee sections were developed by BlueScope Lysaght and the University of Sydney to attain
47 economical beneficiary as well as better structural performance [2]. Pham and Hancock [3]
48 stated that SupaCee sections are performing well compared to conventional CFS channel
49 sections in terms of bending capacity due to their longitudinal web stiffeners as well as return
50 lip stiffeners. Consequently, SupaCee sections replaced general CFS sections in construction
51 applications such as wall studs, roof systems and steel housing frames [3]. Since only a few
52 research investigations in terms of structural performances of SupaCee sections have been
53 carried out, applications of SupaCee sections are limited to some extent. Hence, this study
54 reports the flexural performance of SupaCee sections with and without web openings, as the
55 web openings are essential in a building to accommodate the services such as electrical,
56 plumbing and heating [4]. Fig.2 illustrates the service integration through the web openings of
57 beams in a typical building [5-6].

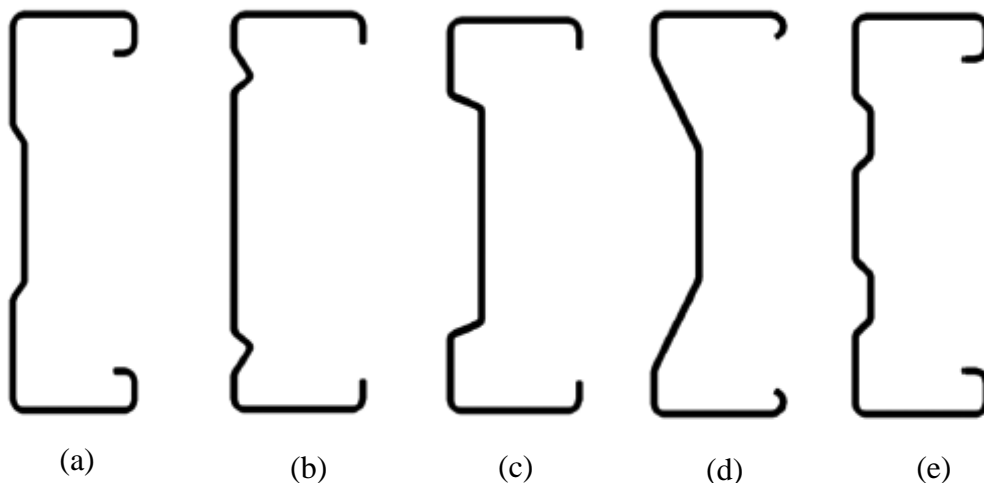


Fig.1: Cross section profiles : (a) DHS (Diamond Hi-Span); (b) Ultra BEAM; (c) Albion Sigma beam; (d) King span; (e) HST [2]

59 Experimental as well as numerical investigations were performed by many researchers to report
60 the flexural behaviour of CFS sections. For example, Yu and Schafer [7] performed
61 experimental distortional buckling tests on CFS sections (C- and Z-sections) under four-point
62 bending to predict the section moment capacities in distortional buckling failure mode. Later,
63 Yu and Schafer [8] performed an extensive numerical study of CFS sections after validating
64 the numerical results against experimental values. Notably, numerical results indicated that
65 existing Direct Strength Method (DSM) based equations were applicable to calculate the
66 distortional and local buckling moments of CFS sections. Further numerical investigations were
67 carried out to analyse the effect of distortional buckling under moment gradient, which was
68 employed by applying the concentrated load at the mid span. An empirical equation was
69 proposed to predict the distortional buckling moment with the influence of moment gradient.
70 Subsequently, Yu and Yan [9] presented an Effective Width Method (EWM) to predict the
71 distortional buckling strength of CFS sections (with C- and Z-profiles) under bending, which
72 exhibited similar performance compared to DSM in terms of accuracy and reliability. Similarly,
73 Kankanamge and Mahendran [10] proposed modified design equations to predict the lateral
74 torsional buckling capacity of Lipped Channel Beam (LCB), whereas Anbarasu [11] presented
75 a modified design equation to calculate elastic distortional buckling moment of LCB sections
76 while the equation was valid only when both distortional and local buckling moments were
77 nearly equal. Meanwhile, a Finite Element (FE) model was developed by Haidarali and
78 Nethercot [12] to analyse the local buckling and combined distortional with local buckling
79 behaviour of laterally restrained CFS sections.



Fig.2: Service integration through web openings [5-6]

80

81 Wang and Young [13] studied the flexural behaviour of CFS sections with stiffened webs and
82 proposed modified DSM equations to predict the flexural capacities of CFS sections with
83 stiffened cross-sections based on the obtained experimental and numerical results. Gatheeshgar
84 et al. [14] investigated the elastic buckling behaviour and flexural performance of Modular

85 Construction Optimised (MCO) beams and proposed new DSM design equations to determine
86 ultimate flexural capacities and elastic buckling moments of MCO beams. Flexural
87 performance of high strength LCB sections and SupaCee sections was experimentally analysed
88 by Pham and Hancock [3]. Twenty-four sections of two different section depths as well as three
89 different thicknesses were considered for the experimental programme. Four-point
90 experimental setup used by Pham and Hancock [3] is shown in Fig.3. The range of 4.5% -
91 22.4% flexural capacity enhancement in SupaCee sections compared to plain C sections was
92 recorded by Pham and Hancock [3] and the reasons stated for the improved flexural capacity
93 were longitudinal stiffeners and return lips which are featured in SupaCee sections. However,
94 extensive numerical studies of flexural performance of SupaCee sections are not reported to till
95 date.

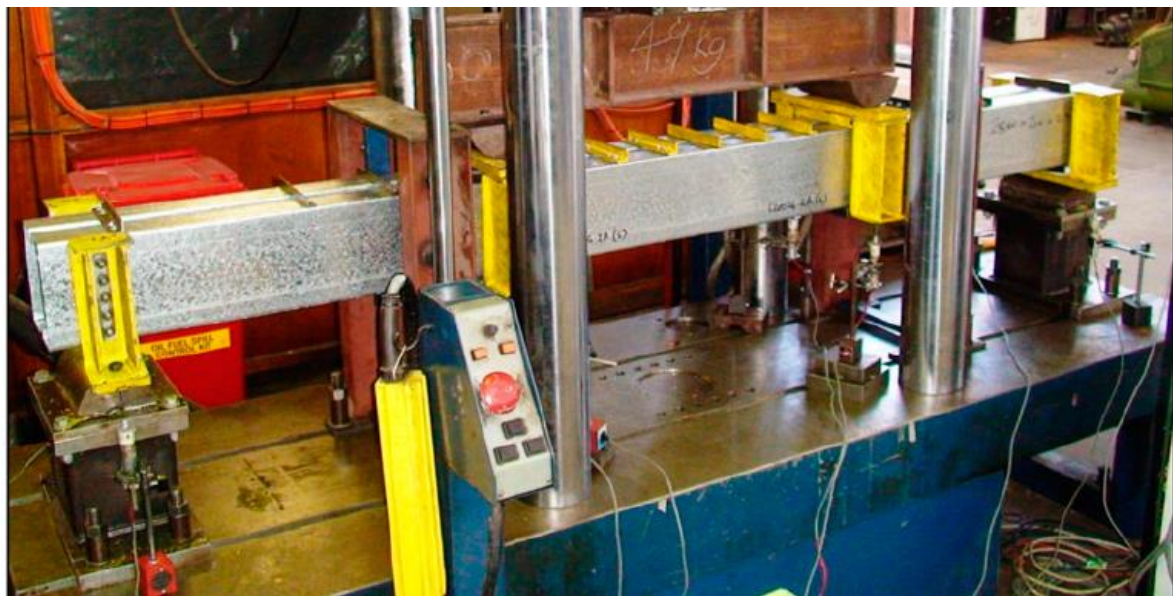


Fig.3: Four-point bending experimental configuration [3]

96

97 Structural behaviour in terms of flexural [4, 15-21], shear [22-31], web crippling [32-41] and
98 web-post buckling [42-43] of CFS sections with web openings is another area where research
99 was conducted considering the web openings in beam sections to integrate electric and
100 hydraulic services. Moen and Schafer [15] investigated the elastic buckling behaviour of CFS
101 sections with web openings and proposed appropriate methods based on the DSM to determine
102 their elastic buckling strengths. Later, Zhao et al. [16] reviewed the flexural performance of
103 CFS sections with web openings and proposed modified formulas based on the DSM to predict
104 their flexural capacities. Yu et al. [17] presented an analytical approach to determine the
105 distortional buckling strength of CFS sections with circular web openings based on the

106 Hancock's [18] method which was proposed to calculate the distortional buckling stress of CFS
107 sections without web openings subjected to pure bending. Chen et al. [4] conducted
108 experimental and numerical analysis on LCB sections with web openings, stiffened web
109 openings and plain webs in terms of flexural performance and compared the results with
110 existing design standards as well as design equations which were proposed earlier by Moen and
111 Schafer [15].

112 Flexural performance of SupaCee sections with web openings should had been analysed as it
113 could display better structural performance compared to other CFS sections due to its cross-
114 section profile. However, the flexural behaviour of SupaCee section with web openings is not
115 explored up to date. In addition, extensive numerical analysis on SupaCee sections with respect
116 to their flexural behaviour is not reported. Hence, this study aims to enhance the applicability
117 of SupaCee sections in the industry by studying their flexural behaviour with openings.
118 Comprehensive numerical studies of flexural behaviour of SupaCee sections with and without
119 the unstiffened web openings is conducted and modified equations with reduction factors are
120 provided to predict the ultimate flexural capacity of SupaCee section with web openings.
121 Moreover, ultimate flexural capacities of SupaCee sections are compared with similar LCB
122 sections and recommendations are stated to replace conventional CFS sections by SupaCee
123 sections with web openings.

124 **2 Numerical Investigation**

125 2.1 Overview

126 The numerical models were developed simulating the actual experimental setup of four-point
127 bending case with the FEA software, ABAQUS [44]. Moreover, developed FE model consists
128 SupaCee section as well as Web Side Plates (WSP). SupaCee sections with and without web
129 openings were modelled using the middle surface offset definition which create the centreline
130 of the section first and then generate the half of the thickness both side of the centreline
131 dimension when applying the section assignments. Therefore, cross-section of the SupaCee
132 section was generated using centre line to generate the actual sections. Besides, relevant
133 material properties such as yield strength, density, Poisson's ratio and elastic modulus were
134 added to the sections. Later, WSPs were assembled to the SupaCee section according to the
135 four-point bending setup using 'tie' constraint which ties beam and WSPs together. Assembly
136 of WSPs to the SupaCee section by using the surface-to-surface 'tie' constraint is illustrated in

137 Fig.4. Master and slave surfaces were chosen during the tie constraint application also
138 mentioned in Fig.4.

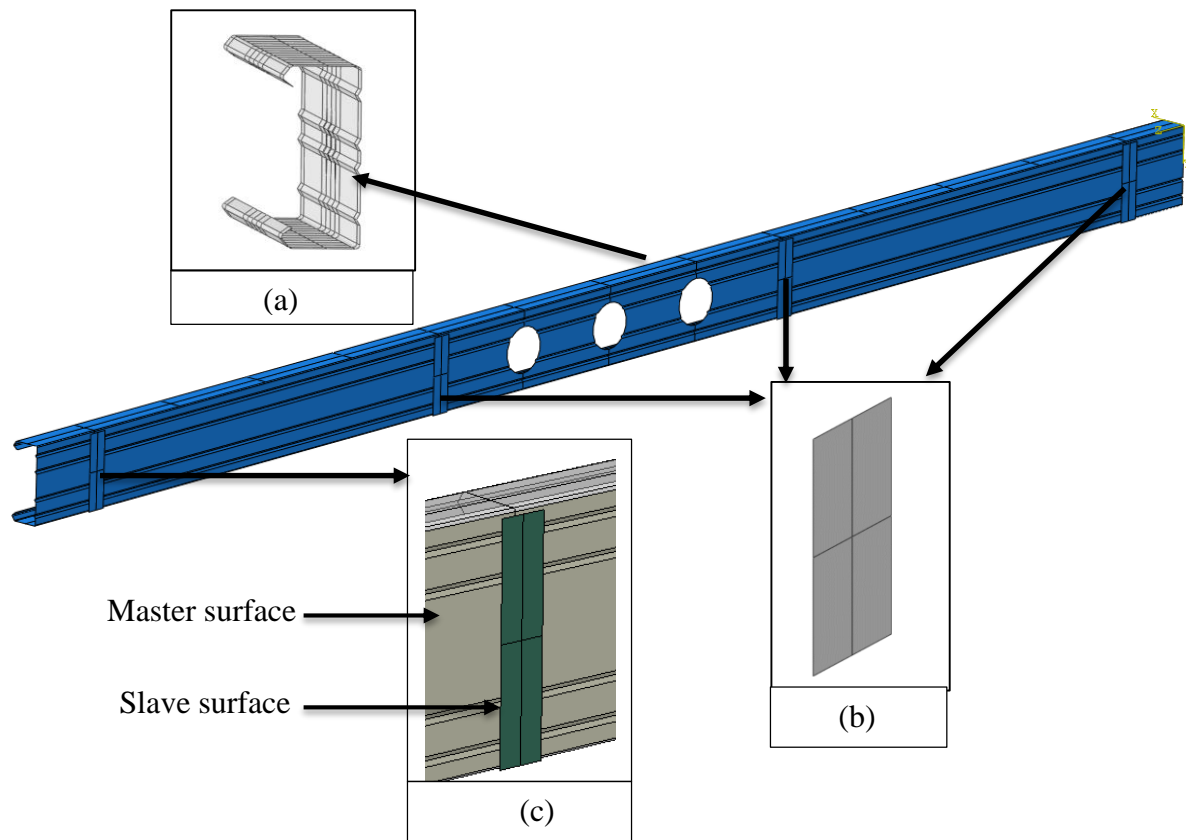


Fig.4: Surface to surface assembly of SupaCee beam and WSP: (a) SupaCee beam (b) WSP and (c) Master and slave surfaces in tie constraint

139

140 The simulation was carried out in two parts: Elastic buckling analysis to attain the eigen modes
141 of the section and non-linear analysis to obtain the failure modes and the ultimate bending
142 capacity. Buckling modes from the former analysis was used to add the initial geometric
143 imperfection while performing non-linear analysis to stimulate the out-of-plane deformations
144 of the section elements. Imperfection magnitude of $0.15t$ where t is the thickness of the section,
145 was used in the numerical simulations as it was recommended by Pham and Hancock [45].
146 Comparison of obtained numerical results against experimental outcomes was stated by Pham
147 and Hancock [45]. The comparison was done by changing the imperfection magnitudes as well
148 as corresponding eigen modes and $0.15t$ imperfection magnitude was found appropriate for
149 accurate replication of experimental condition. The static general analysis was employed with
150 non-linear analysis after taking in to the consideration of validation procedure and previous
151 similar work [46]. A comprehensive description regarding the numerical analysis of flexural
152 behaviour of the SupaCee sections with openings is provided next.

153 2.2 Element type and meshing scheme

154 S4R shell element type was opted to model the SupaCee section as its thickness was negligible
155 compared to other dimensions, whereas R3D4 rigid element was selected for WSP to represent
156 the rigid nature of WSP. Similar several research studies [36-39, 46] employed S4R element
157 type due to its merits such as accuracy, reduced integration and lesser-required time. Hence,
158 four-node S4R shell element was preferred over other shell element types available in
159 ABAQUS.

160 Meshing scheme was selected by considering similar research studies [36-39, 46] and the
161 results from the mesh sensitivity analysis. 5 mm x 5 mm mesh size was provided to SupaCee
162 section with and without openings. However, Corner regions of the section were refined by
163 finer mesh size of 1 mm x 5 mm to neglect the effects on ultimate strength due to the curvature
164 of the section. Similar concept was considered by Perera and Mahendran [47] in the corner
165 sections. Subsequently, coarse mesh size of 10 mm x 10 mm was selected for the WSP. In
166 addition, mesh control with medial axis algorithm was applied to ensure the smooth mesh
167 pattern near web openings. Provided meshing scheme for the FE model is illustrated in Fig.5.

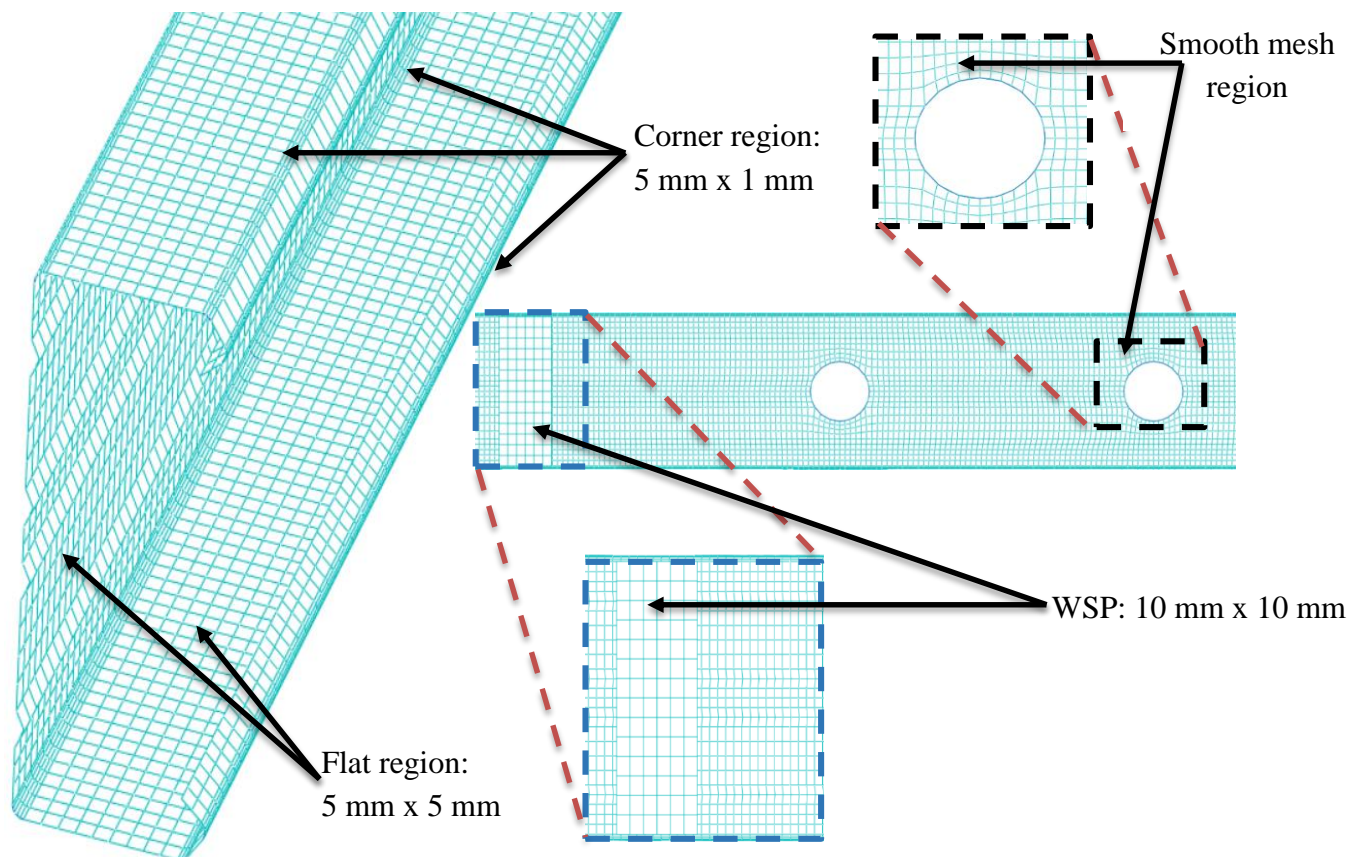


Fig.5: Mesh scheme of the numerical study

169 2.3 Material model

170 Selection of material characteristics of SupaCee section is significant in the numerical analysis
171 considering the accuracy of the obtained ultimate bending capacities and failure modes. Stress-
172 strain behaviour of CFS was used in the numerical modelling with negligible strain hardening
173 based on the past studies [36-39, 48]. Besides, elastic perfectly plastic material model with
174 nominal yield strength was employed. Corner strength enhancement and residual stress were
175 neglected in the analysis as they compensate each other [49]. SupaCee section was modelled
176 with the density, elastic modulus and Poisson's ratio values of 7850 kg/m^3 , 200 GPa and 0.3,
177 respectively.

178 2.4 Boundary condition and load application

179 Four-point bending setup was selected for the numerical analysis to ensure the failure is purely
180 bending at the mid-span where the ultimate bending capacities would be obtained. Reference
181 points were added in the WSPs to assign the load and boundary conditions. Simply supported
182 boundary conditions and loading conditions were employed at the reference points of WSPs
183 using displacement control method. Moreover, lateral restraints were added in the SupaCee
184 section at the centre of top and bottom flanges in 300 mm intervals to eliminate lateral torsional
185 and distortional buckling and to ensure the local buckling failure in the beam. Fig.6 depicts the
186 assigned boundary conditions and loading application of the SupaCee section. Load application
187 properties such as maximum load increments (1000), initial increment size (0.01), total time
188 period (1.0), minimum increment size (1×10^{-25}) and maximum increment size (0.1) were
189 selected based on the previous numerical studies [36-39].

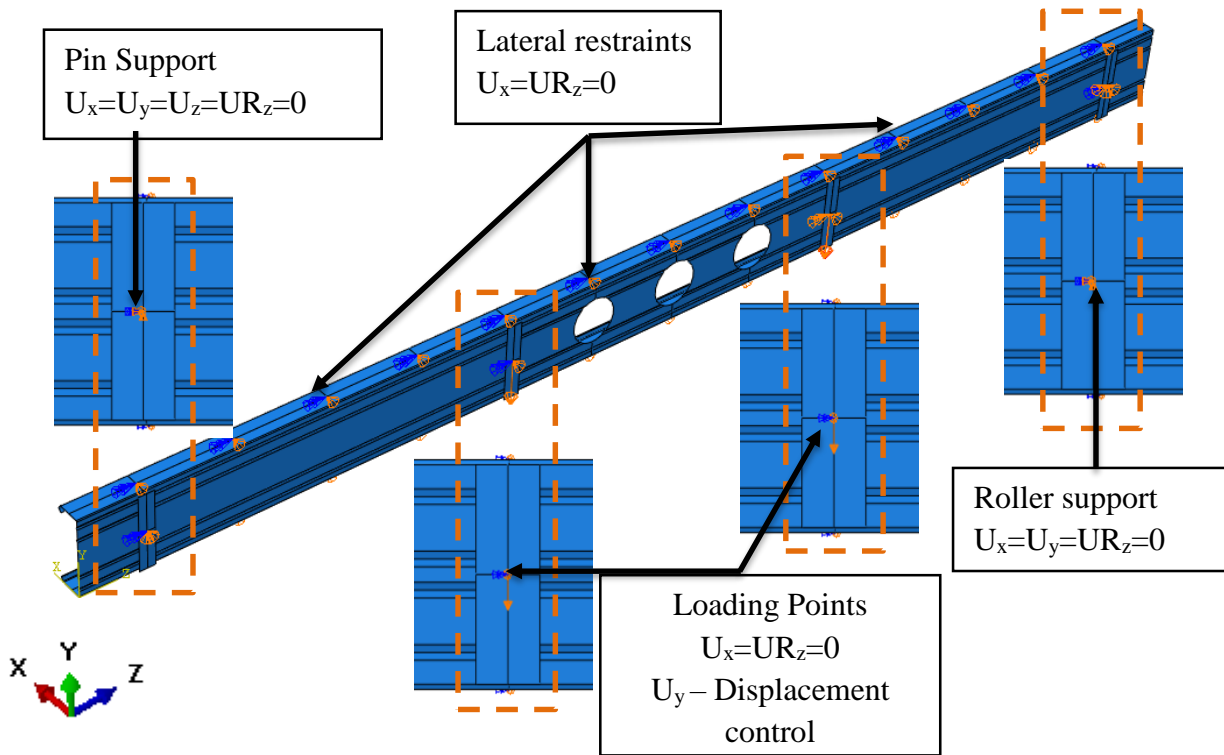


Fig.6: Applied boundary conditions and loading terms

191 3.1 Validation of FE model

192 Validation is mandatory before numerical analysis as it is important to ensure the reliability of
 193 the results from the parametric study. Hence, through the validation procedure, selected
 194 modelling features including element types, meshing scheme, material properties, boundary
 195 conditions, imperfections and non-linear analysis method can be justified. Experimental results
 196 from the Pham and Hancock’s study [3] on SupaCee sections were taken for the validation of
 197 the numerical analysis which investigates the flexural behaviour of SupaCee section with web
 198 openings. Pham and Hancock [3] conducted experiments on SupaCee section with two different
 199 section depths (150 mm and 200 mm) and three different thicknesses (1.2 mm, 1.5 mm and 2.4
 200 mm). Altogether six experimental results were taken in-to consideration for the validation and
 201 Table 1 shows validation results and the comparison between FEA and experimental results.

Table 1: Comparison of FE results against experimental results

Section	Sectional depth (d)	Thickness of section (t)	Material yield strength (f_y)	Experiment results [3]	FEA values	Experiment/FEA
	(mm)	(mm)	(MPa)	(kNm)	(kNm)	
SC15012	150	1.2	589.71	8.19	7.97	1.03
SC15015	150	1.5	533.88	11.40	9.98	1.14
SC15024	150	2.4	513.68	21.19	19.91	1.06
SC20012	200	1.2	593.30	10.71	10.04	1.07
SC20015	200	1.5	532.03	16.48	14.89	1.11
SC20024	200	2.4	504.99	33.82	29.79	1.14
Mean						1.09
COV						0.04

203 Obtained FEA results against experimental results shown good agreement with the mean value
 204 of 1.09 and Coefficient of Variation (COV) value of 0.04. Subsequently, failure mode and load
 205 vs deflection curve of the experimental section and FE model were compared. Results of both
 206 comparisons are illustrated in Fig.7 and Fig.8, respectively. Both Comparisons reported a good
 207 resemblance between FE model and the experimental setup.

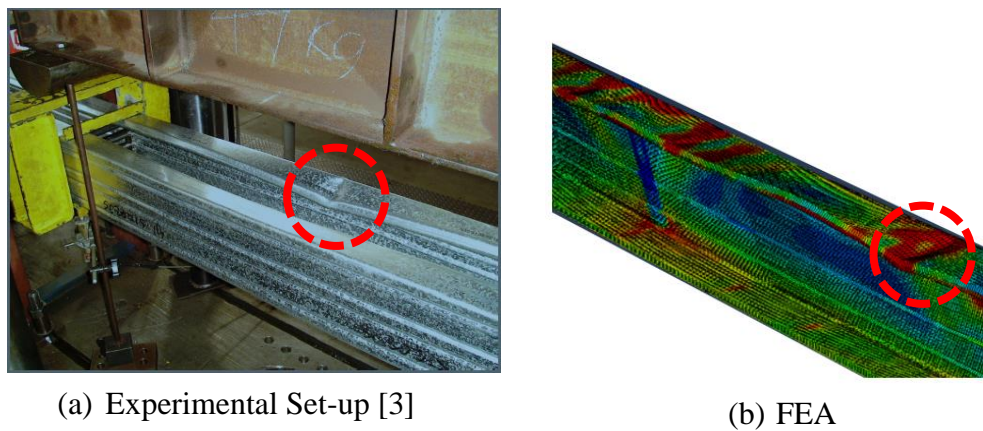


Fig.7: Failure pattern comparison for SC20015 [3]

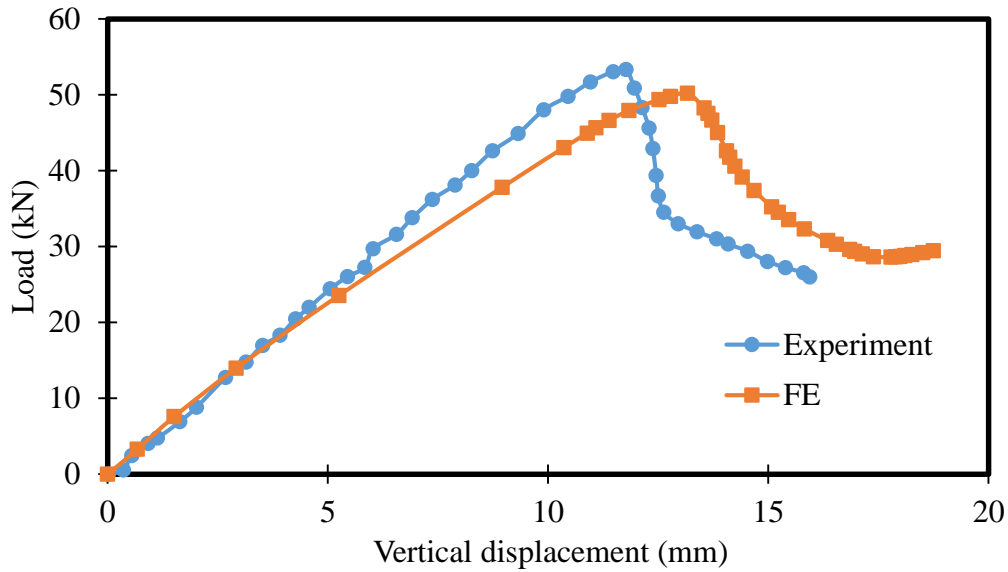


Fig. 8: Load vs. deflection curve for section SC20012 [3]

209

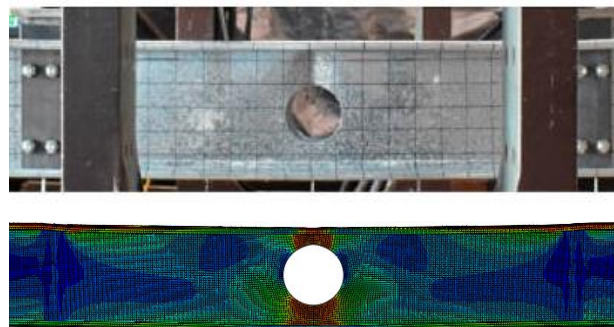
210 Similarly, validation procedure was conducted to verify the FE models with web openings
 211 against experimental results. Research work from Chen et al. [4] in the flexural behaviour of
 212 CFS sections (Lipped Channel Beam (LCB)) with and without web openings was taken for the
 213 validation purpose. Validation results are stated in Table 2 and the comparison indicated good
 214 agreement between FEA and test results with the mean value of 0.95 and COV value of 0.05.
 215 Fig.9 and Fig.10 illustrates the failure mode and load vs. deflection curve comparisons which
 216 also showed a good agreement of the FE results. Since developed models using ABAQUS
 217 predicted the flexural behaviour of SupaCee sections without openings and LCB sections
 218 accurately, the developed numerical model was taken in to consideration for the parametric
 219 studies. This numerical approach ensures the effect of web stiffeners and return lips by
 220 validating the SupaCee section without web openings and effect of web openings by validating
 221 LCB sections. Besides, the similar numerical combination approach was followed in similar
 222 studies earlier [31]. Hence, based on the validation process, results and comparisons, developed
 223 numerical model was selected to carry out the parametric study and to analyse the flexural
 224 behaviour of SupaCee sections with web openings.

225

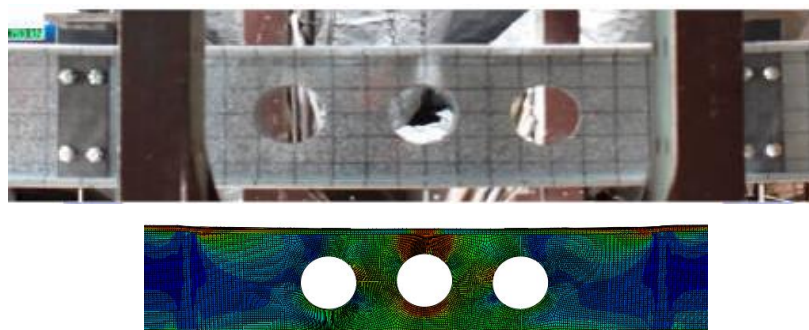
Table 2: Comparison of section moment capacity between FE results and test [4]

Specimen	Hole diameter (mm)	Hole spacing (mm)	Test [4] (kNm)	FE (kNm)	Test/FE
Plain section					
240-L4000-NH	–	–	11.90	11.63	1.02
290-L4000-NH	–	–	18.00	19.15	0.94
Un-stiffened web openings					
240-L4000-UH1	141.5	–	11.00	11.25	0.98
240-L4000-UH3	140.8	100	10.60	11.20	0.95
290-L4000-UH1	141.5	–	16.70	18.74	0.89
290-L4000-UH3	141.9	100	16.30	17.90	0.91
Mean					0.95
COV					0.05

226



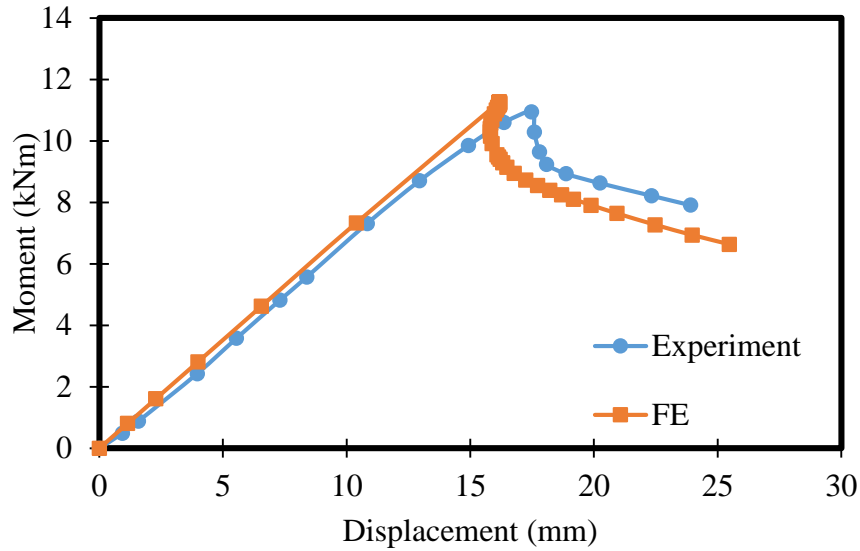
(a)



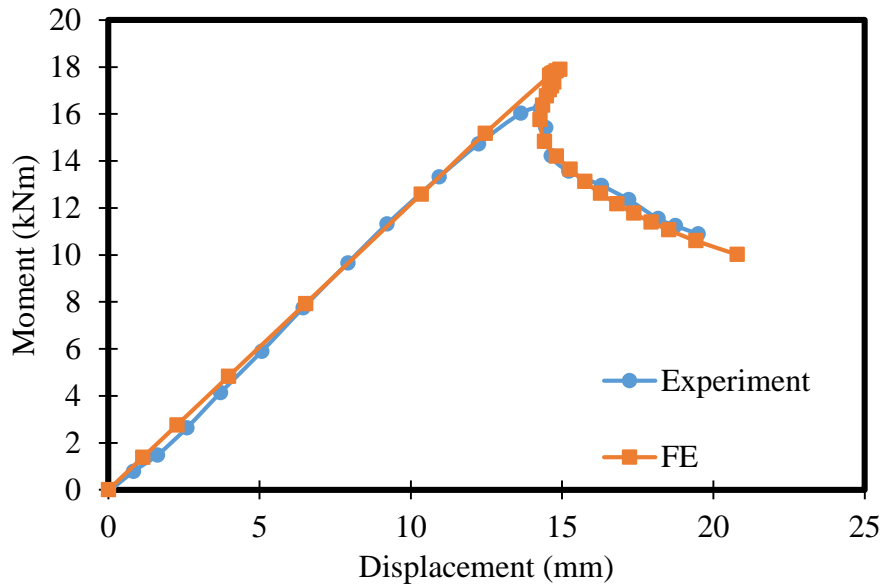
(b)

Fig.9: Failure Pattern Comparison of section: (a) 240-L4000-UH1; (b) 290-L4000-UH3 [4]

227



(a)



(b)

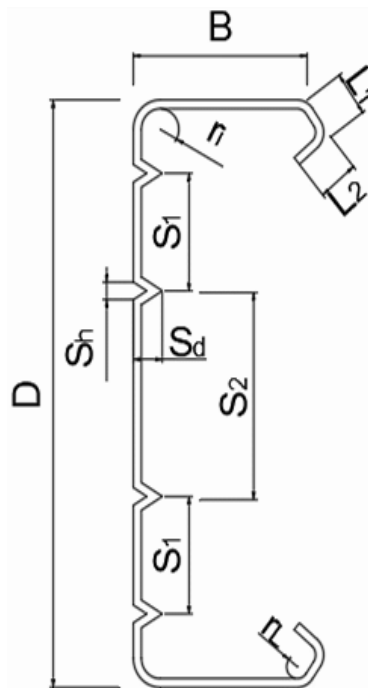
Fig.10: Comparison of moment vs. displacement curve for sections: (a) 240-L4000-UH1 and (b) 290-L4000-UH3

228

229 3.2 Parametric plan

230 Parametric plan to carry out an extensive study on the flexural performance of SupaCee sections
 231 with web openings was developed based on the critical parameters after the validation process
 232 of numerical models. Accordingly, three various section depths (150 mm, 200 mm and 250
 233 mm) and three different thicknesses (1 mm, 2 mm and 2.5 mm) were selected as the key
 234 dimensions of the SupaCee section. Parametric dimensions of the SupaCee section are provided
 235 in Fig.11 and Table 3.

236 Web opening ratios (d_{wh}/d_1) were selected as 0.0, 0.4, 0.6 and 0.8 and material yield strengths
 237 were considered as 300 MPa, 450 MPa and 600 MPa. Industrial requirements and previous
 238 studies [27, 36, 38, 48] were considered to select the web opening sizes and stress-strain
 239 behaviour was opted based on elastic perfectly plastic model as described earlier. In addition,
 240 effect of spacing between web openings was considered in this study. Hence, two different
 241 spacing (300 mm and 450 mm) were planned to provide between the web openings which
 242 dimension considered between web opening centres. Parametric plan was drafted considering
 243 all afore mentioned parameters and provided in Table 4. Overall, 189 FE models were planned
 244 to analyse the flexural performance of SupaCee section with and without web openings in this
 245 study.



246 Fig. 11: Cross-section profile of SupaCee beam

247

247 Table 3: Selected dimensions of SupaCee section

H (mm)	B (mm)	L ₁ & L ₂ (mm)	a ₁ (mm)	a ₂ (mm)	S ₁ (mm)	S ₂ (mm)	S _h (mm)	S _d (mm)	r _i & r ₁ (mm)
150	50	12	125	95	40	20	10	5	2
200	65	15	125	95	40	70	10	5	2
250	75	15	125	95	40	120	10	5	2

Table 4: Parametric plan

Section	Thickness	web hole diameter ratio	Hole spacing	Strength	No. of Models
H x B (mm x mm)	t (mm)	d_{wh}/d_1	S (mm)	f_y (MPa)	
Plain section					
150 × 50	1, 2, 2.5	0	-	300, 450, 600	9
200 × 65	1, 2, 2.5	0	-	300, 450, 600	9
250 × 75	1, 2, 2.5	0	-	300, 450, 600	9
Un-stiffened web openings					
150 × 50	1, 2, 2.5	0.4, 0.6, 0.8	300, 450	300, 450, 600	54
200 × 65	1, 2, 2.5	0.4, 0.6, 0.8	300, 450	300, 450, 600	54
250 × 75	1, 2, 2.5	0.4, 0.6, 0.8	300, 450	300, 450, 600	54
Total					189

249 4 Results and Discussion

250 Detailed numerical analysis was carried out based on the results from the comprehensive
 251 parametric study are provided and discussed in this chapter. Table.5 outlines the obtained
 252 ultimate bending capacities (M) with corresponding web opening ratios (d_{wh}/d_1), hole spacing
 253 (S), thickness (t) and yield strengths (f_y).

254 Table.5: Parametric study results

H	t	d_{wh}/d_1	S = 300 mm			S = 450 mm		
			$f_y = 300$ MPa	$f_y = 450$ MPa	$f_y = 600$ MPa	$f_y = 300$ MPa	$f_y = 450$ MPa	$f_y = 600$ MPa
(mm)	(mm)		M (kNm)	M (kNm)	M (kNm)	M (kNm)	M (kNm)	M (kNm)
150	1	0	4.12	5.89	7.23	4.12	5.89	7.23
150	1	0.4	2.95	4.48	5.73	2.88	4.42	5.29
150	1	0.6	2.83	4.26	5.30	2.52	3.91	5.11
150	1	0.8	1.95	2.93	3.65	1.38	2.36	3.10
150	2	0	9.05	13.05	17.07	9.05	13.05	17.07
150	2	0.4	7.00	11.41	15.15	6.89	11.09	14.78
150	2	0.6	6.78	10.84	14.46	6.25	10.27	14.02
150	2	0.8	4.88	7.95	10.82	4.08	7.08	10.01
150	2.5	0	10.01	16.04	22.15	10.01	16.04	22.15
150	2.5	0.4	8.69	14.38	19.79	8.58	13.87	18.66
150	2.5	0.6	8.36	13.57	18.13	7.76	12.74	17.63
150	2.5	0.8	6.15	10.00	13.71	5.17	8.93	12.64
200	1	0	6.04	9.11	9.54	6.04	9.11	9.54
200	1	0.4	4.14	5.88	6.93	4.05	5.83	6.41

200	1	0.6	4.05	5.77	5.89	3.54	5.13	5.37
200	1	0.8	3.21	4.53	5.56	2.63	3.94	4.96
200	2	0	12.98	21.89	29.02	12.98	21.89	29.02
200	2	0.4	10.80	17.05	21.25	10.70	16.38	21.17
200	2	0.6	10.56	16.80	20.60	9.64	15.26	20.00
200	2	0.8	8.68	13.56	17.26	7.55	12.18	16.41
200	2.5	0	17.05	27.05	35.89	17.05	27.05	35.89
200	2.5	0.4	13.69	21.57	28.57	13.46	21.07	27.91
200	2.5	0.6	12.98	21.03	27.58	12.03	19.30	26.03
200	2.5	0.8	11.02	17.02	23.41	9.72	16.02	21.91
250	1	0	9.55	11.11	13.44	9.55	11.11	13.44
250	1	0.4	7.01	9.55	11.39	6.99	9.57	11.34
250	1	0.6	6.90	8.98	10.44	6.24	8.47	10.30
250	1	0.8	5.81	7.85	9.48	5.14	7.36	9.16
250	2	0	19.05	28.85	38.20	19.05	28.85	38.20
250	2	0.4	18.57	27.92	35.22	18.33	27.85	34.73
250	2	0.6	18.09	26.77	32.46	16.61	25.07	31.93
250	2	0.8	15.13	22.73	28.88	13.74	20.87	27.15
250	2.5	0	26.08	38.40	54.02	26.08	38.40	54.02
250	2.5	0.4	24.63	37.08	51.46	24.12	36.89	48.23
250	2.5	0.6	23.85	35.31	45.46	21.34	33.87	43.49
250	2.5	0.8	19.45	30.10	39.92	17.50	28.34	37.93

255 Fig.12 illustrates the failure modes of section 150×50×1 ($d_{wh}/d_1 = 0.4$) at various stages with
256 load-deflection curve obtained from the numerical analysis. Moreover, initial imperfection
257 contour of the same section is illustrated in Fig.12. Meanwhile, Fig.13 compares the load-
258 deflection curve of section 150×50×2 ($d_{wh}/d_1 = 0.4$) with hole spacing (300 mm and 450 mm).
259 Based on the results, it can be stated that hole spacing has little impact on the ultimate bending
260 capacity of SupaCee sections with web openings and the results indicated that lesser space
261 between web openings is beneficial in terms of flexural capacity.

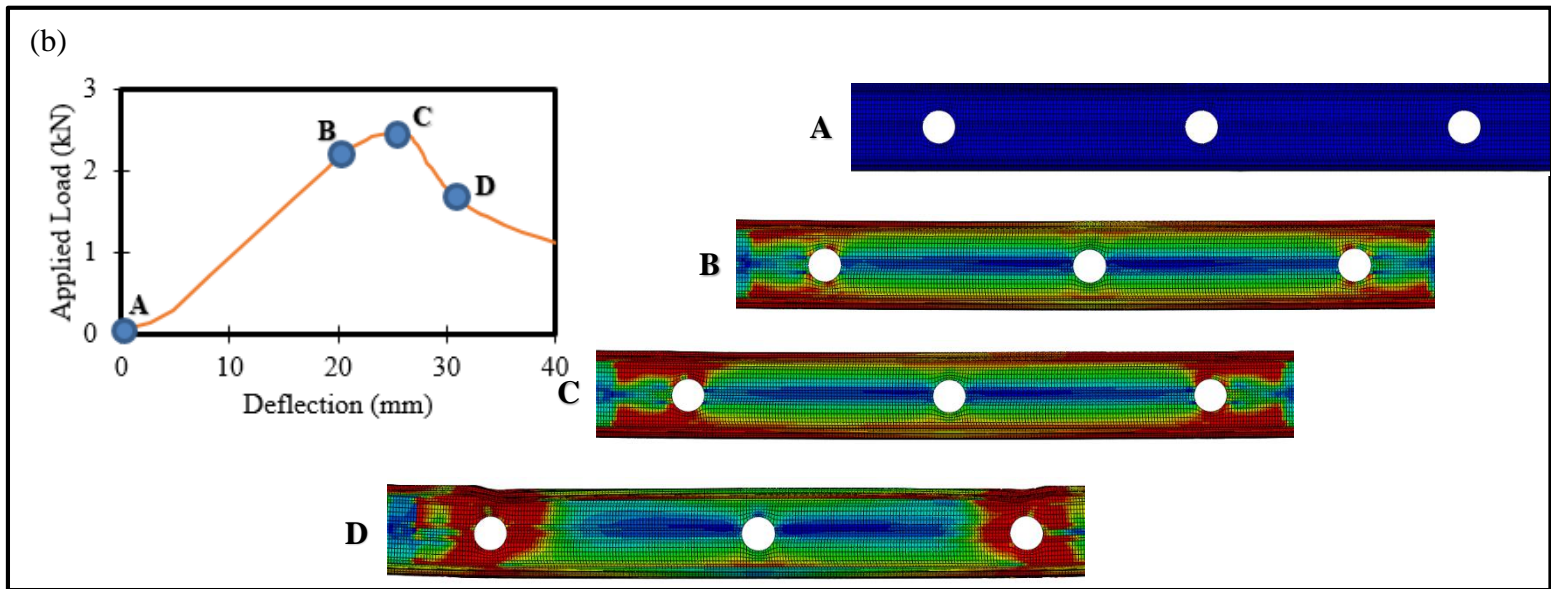
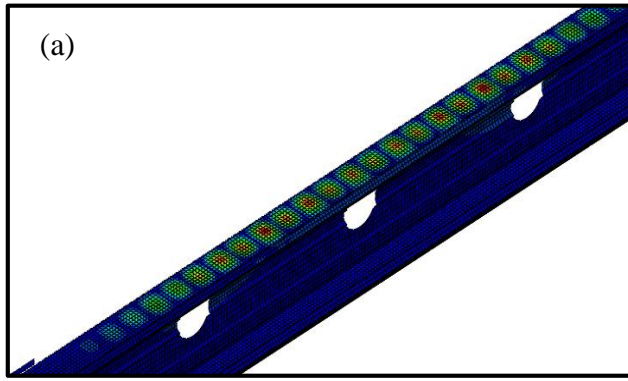


Fig.12: (a) Initial imperfection contours and (b) failure modes of section 150x50x1 ($d_{wh}/d_1 = 0.4$)

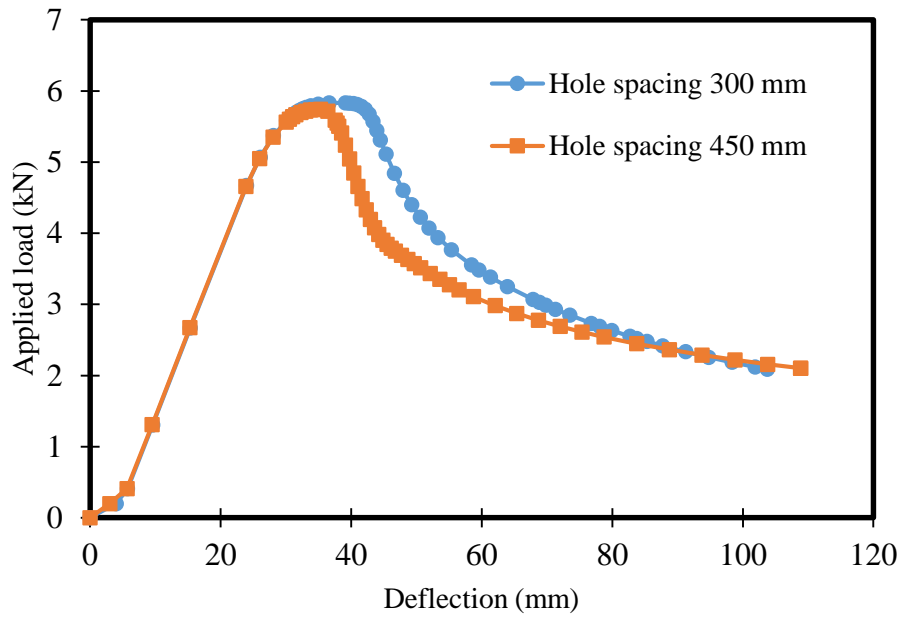


Fig.13: Load vs deflection curve comparison (150x50x2) with hole spacing

263

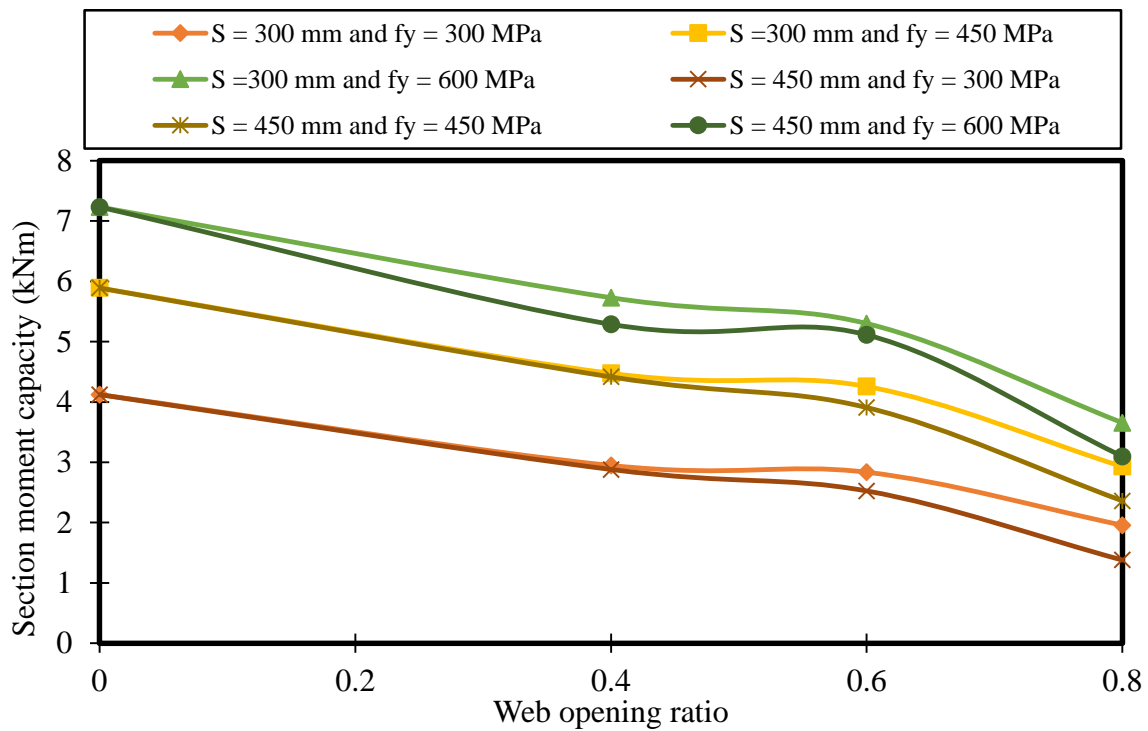


Fig.14: Comparison of flexural capacities with hole spacing (S) and yield strength (f_y) for 150 mm section ($t = 1$ mm)

264

265 Fig.15 shows flexural capacity variation with respect to thickness of different sections with web
 266 openings. Comparison indicates that increase in thickness will improve the flexural capacity of
 267 SupaCee section. Similarly, Fig.16 demonstrates the impact of yield strength in flexural
 268 capacity of SupaCee sections with web openings and high yield strength section shows

269 improved bending capacity. Moreover, Fig.17 compares the load vs. deflection curve obtained
 270 of the 200 mm section for different web opening ratios, where a sudden drop is evident in web
 271 opening ratio of 0.8. Reduction area in web stiffeners due to web openings is lesser in web
 272 opening ratios of 0.4 and 0.6, whereas in web opening ratio of 0.8 reduction area is higher as it
 273 cut through all four web stiffeners in the SupaCee section. Hence, a significant decline is
 274 observed in between web opening ratio of 0.6 to 0.8. Fig.18 displays the failure patterns for the
 275 corresponding sections respectively.

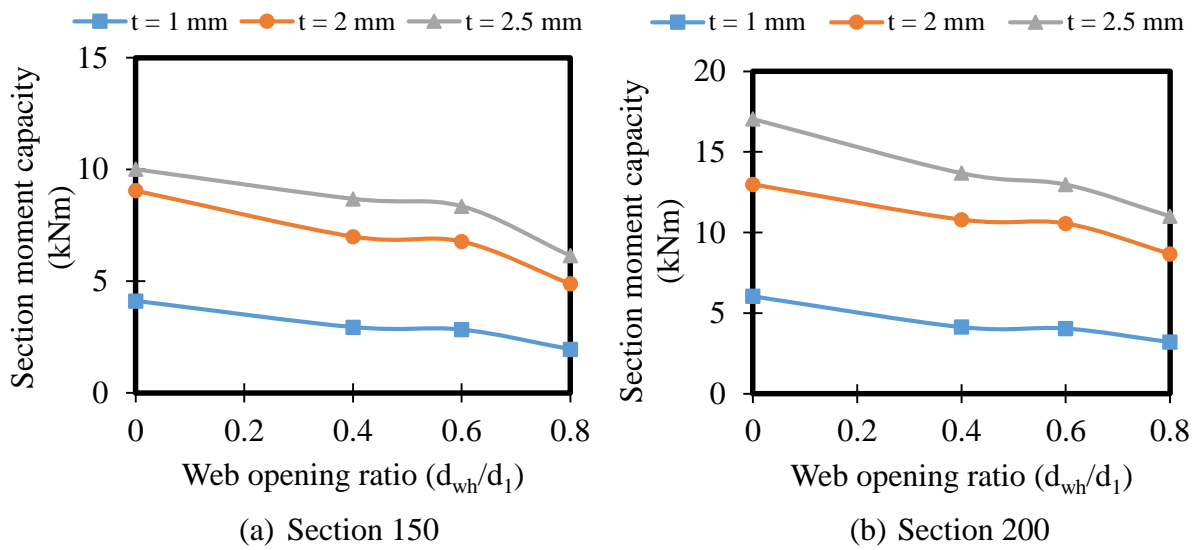


Fig.15: Comparison of flexural capacities with thickness ($f_y = 300$ MPa)

276

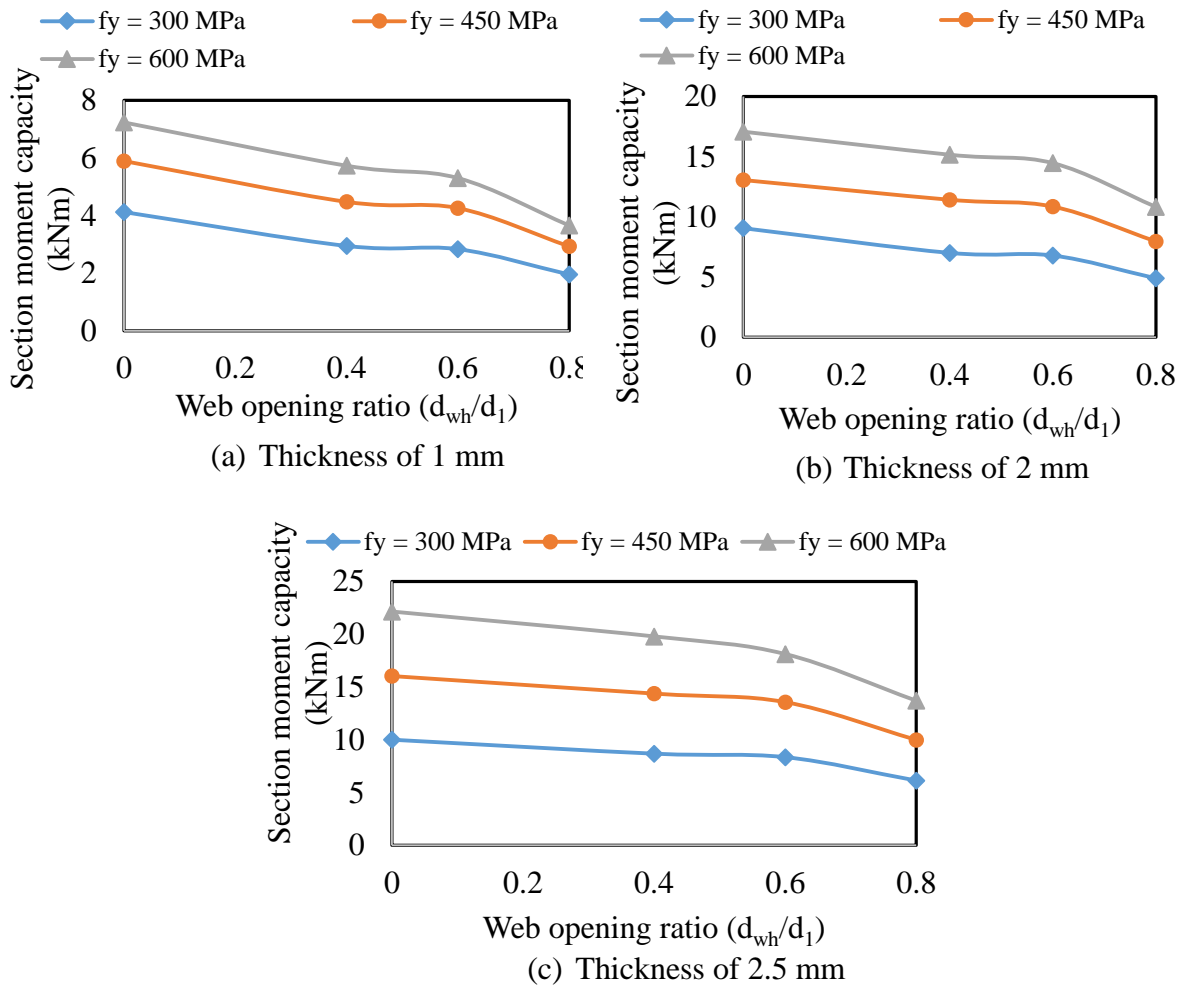


Fig.16: Comparison of flexural capacities with yield strength (Section 150)

277

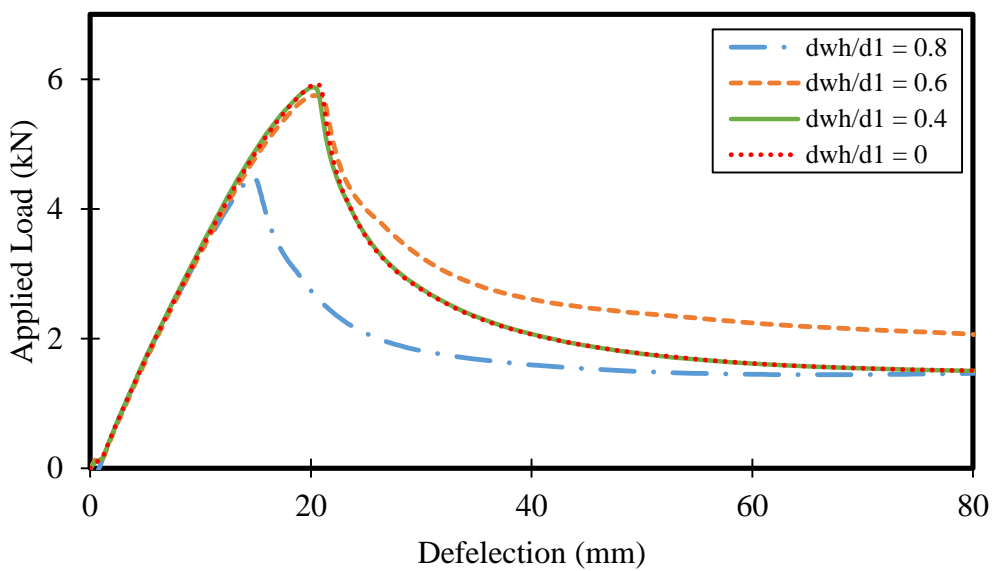


Fig.17: Load vs. deflection curve comparison with web opening ratio

278

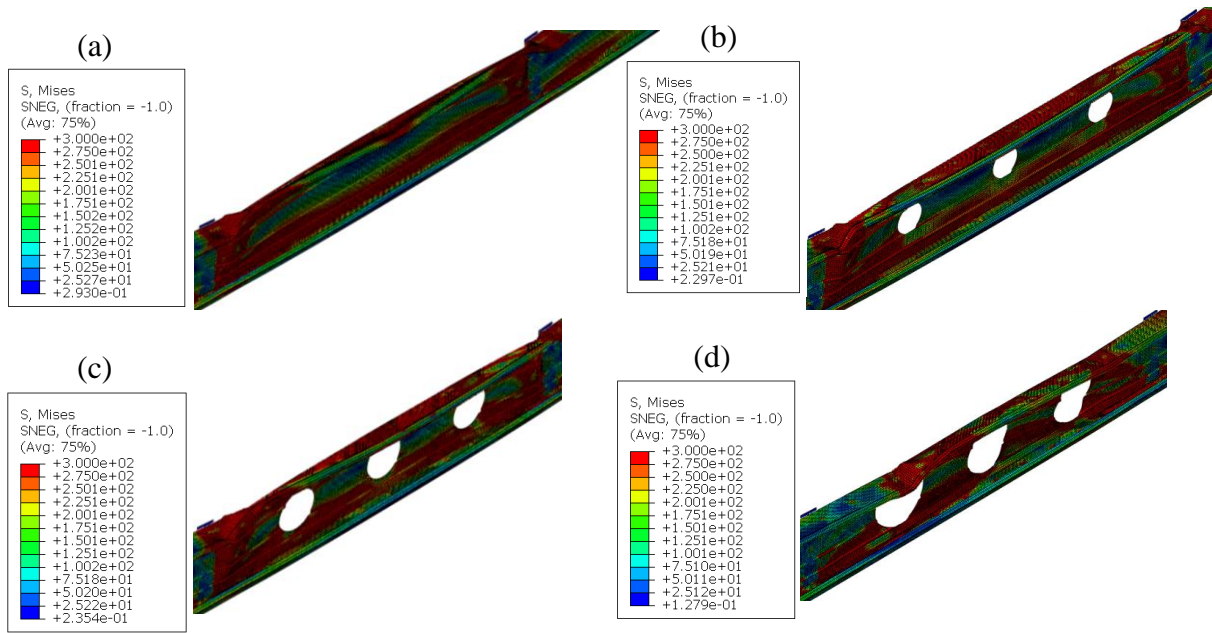


Fig.18: Failure mode comparison with various web opening ratio: (a) $d_{wh}/d_1 = 0$;
 (b) $d_{wh}/d_1 = 0.4$; (c) $d_{wh}/d_1 = 0.6$; (d) $d_{wh}/d_1 = 0.8$

279

280 5 Current design rules for flexural behaviour

281 This section reviews the existing design equations in previous research works on CFS sections
 282 as well as design standards such as AISI S100 [50] and AS/NZS 4600 [51] to calculate the
 283 flexural capacity of CFS sections without web openings and the proposed design formulas in
 284 the literature [3, 15-16] for section moment capacity of CFS sections with web openings.

285 AISI S100 [50] and AS/NZS 4600 [51] provide the following equations (Eqs. (1) – (3)) to
 286 predict the nominal moment capacity (M_{nl}) of CFS sections at local buckling.

$$M_{nl} = M_{ne} \quad \text{for } \lambda_l \leq 0.776 \quad (1)$$

$$M_{nl} = \left[1 - 0.15 \left(\frac{M_{crl}}{M_{ne}} \right)^{0.4} \right] \left(\frac{M_{crl}}{M_{ne}} \right)^{0.4} M_{ne} \quad \text{for } \lambda_l > 0.776 \quad (2)$$

$$\lambda_l = \sqrt{\frac{M_{ne}}{M_{crl}}} \quad (3)$$

287 Where, M_{nl} - nominal member moment capacity at local buckling; M_{ne} - nominal member
 288 flexural strength for lateral torsional buckling; M_{crl} - critical elastic buckling moment; λ_l - non-
 289 dimensional slenderness value for local buckling.

290 Eqs. (4) – (6) from AISI S100 [50] and AS/NZS 4600 [51] can be used to calculate the nominal
 291 moment capacity (M_{nd}) of CFS sections at distortional buckling.

$$M_{nd} = M_y \quad \text{for } \lambda_d \leq 0.673 \quad (4)$$

$$M_{nd} = \left[1 - 0.22 \left(\frac{M_{crd}}{M_y} \right)^{0.5} \right] \left(\frac{M_{crd}}{M_y} \right)^{0.5} M_y \quad \text{for } \lambda_d > 0.673 \quad (5)$$

$$\lambda_d = \sqrt{\frac{M_y}{M_{crd}}} \quad (6)$$

292 Where, M_{nd} - nominal member moment capacity for distortional buckling; M_y - member yield
 293 moment ($M_y = S_f \times f_y$, S_f - section modulus; f_y - elastic distortional buckling stress); M_{crd} -
 294 critical elastic distortional buckling moment; λ_d - non-dimensional slenderness value for
 295 distortional buckling.

296 Shifferaw and Schafer [52] provided a general method to address the inelastic bending capacity
 297 of CFS sections based on the experimental and numerical data. The relationship of inelastic
 298 local buckling and lateral torsional buckling is provided by Eqs. (7) – (11) which were verified
 299 by Shifferaw and Schafer [52]. Later, Pham and Hancock [3] proposed equation (Eq. (12)) to
 300 predict inelastic local buckling and distortional buckling for extended slender sections.
 301 Moreover, Pham and Hancock [3] reported that existing design equations to predict the flexural
 302 capacities of CFS sections can be also applicable to SupaCee sections.

$$M_n = M_y + \left(1 - \frac{1}{C_y^2} \right) (M_p - M_y) \quad \text{for } \lambda_d \leq 0.673, \quad \lambda_l \leq 0.776 \quad (7)$$

$$\lambda_d = \sqrt{\frac{M_y}{M_{crd}}} \quad (8)$$

$$\lambda_l = \sqrt{\frac{M_y}{M_{crl}}} \quad (9)$$

$$C_{yd} = \sqrt{\frac{0.673}{\lambda_d}} \leq 3 \quad (10)$$

$$C_{yl} = \sqrt{\frac{0.776}{\lambda_l}} \leq 3 \quad (11)$$

$$M_{ny} = M_y + \left(1 - \frac{1}{C_y^2}\right)(M_p - M_y) \quad \text{for } \lambda_d \leq 1.45, \quad \lambda_l \leq 1.55 \quad (12)$$

303 Where, λ_l and λ_d – non-dimensional slenderness values; M_y – yield moment; M_p – plastic
 304 moment; M_{ny} – inelastic moment for extended slenderness limit; C_{yl} - local yield strain
 305 multiplier; C_{yd} – distortional yield strain multiplier

306 Moen and Schafer [15] investigated the flexural behaviour of CFS sections with web openings
 307 and proposed design equations to predict ultimate flexural strength based on the DSM which
 308 includes the influence of web openings. The equations were proposed for limit states including
 309 local and distortional buckling. The nominal flexural capacity for local buckling (M_{nl}) of CFS
 310 sections with unstiffened web openings can be calculated using Eqs. (13) – (16).

$$M_{nl} = M_{ne} \leq M_{ynet} \quad \text{for } \lambda_l \leq 0.776 \quad (13)$$

$$M_{nl} = \left[1 - 0.15 \left(\frac{M_{crl}}{M_{ne}}\right)^{0.4}\right] \left(\frac{M_{crl}}{M_{ne}}\right)^{0.4} M_{ne} \leq M_{ynet} \quad \text{for } \lambda_l > 0.776 \quad (14)$$

$$\lambda_l = \sqrt{\frac{M_{ne}}{M_{crl}}} \quad (15)$$

$$M_{crl} = \min(M_{crlg}, M_{crlh}) \quad (16)$$

311 Where, M_{ni} - nominal flexural capacity of local buckling; M_{ynet} - member yield moment
 312 capacity of net cross-section; M_{crl} - critical elastic local moment (considering the influence of
 313 web openings); M_{ne} - nominal section moment capacity for lateral torsional buckling; M_{crlg} -
 314 critical elastic buckling moment at gross cross-section; M_{crlh} - critical local buckling moment
 315 of compressed section above the web opening; λ_l - non-dimensional slenderness value for local
 316 buckling.

317 DSM based design equations (Eqs. (17) - (24)) to calculate the nominal moment capacity for
 318 distortional buckling of CFS sections with web openings were proposed by Moen and Schafer
 319 [15].

$$M_{nd} = M_{ynet} \quad \text{for } \lambda_d \leq \lambda_{d1} \quad (17)$$

$$M_{nd} = M_{ynet} - \left(\frac{M_{ynet} - M_{d2}}{\lambda_{d2} - \lambda_{d1}} \right) (\lambda_d - \lambda_{d1}) \quad \text{for } \lambda_{d1} < \lambda_d \leq \lambda_{d2} \quad (18)$$

$$M_{nd} = \left[1 - 0.22 \left(\frac{M_{crd}}{M_y} \right)^{0.5} \right] \left(\frac{M_{crd}}{M_y} \right)^{0.5} M_y \quad \text{for } \lambda_d > \lambda_{d2} \quad (19)$$

$$\lambda_d = \sqrt{\frac{M_y}{M_{crd}}} \quad (20)$$

$$\lambda_{d1} = 0.673 \left(\frac{M_{ynet}}{M_y} \right)^3 \quad (21)$$

$$\lambda_{d2} = 0.673 \left[1.7 \left(\frac{M_y}{M_{ynet}} \right)^{2.7} - 0.7 \right] \quad (22)$$

$$M_{d2} = \left(1 - 0.22 \left(\frac{1}{\lambda_{d2}} \right) \right) \left(\frac{1}{\lambda_{d2}} \right) M_y \quad (23)$$

$$M_{crd} = \min(M_{crdg}, M_{crdn}) \quad (24)$$

320 Where, M_{nd} — section moment capacity for distortional buckling; M_{ynet} - member yield moment
321 of net cross-section; M_{crd} - critical elastic distortional buckling moment (including the effect of
322 web openings); M_{crdg} - critical elastic distortional buckling moment of gross cross-section;
323 M_{crdn} - critical elastic distortional buckling moment at a web opening; M_y - member yield
324 moment; λ_{d1} , λ_d and λ_{d2} - non-dimensional slenderness values.

325 Zhao et al. [16] modified existing design equations to predict the flexural capacity of CFS
326 sections with web openings as it was found that web openings were influencing failure modes
327 by changing the failure modes from only local buckling or only distortional buckling to local-
328 distortional buckling interaction controlled by local buckling or distortional-local buckling
329 interaction controlled by distortional buckling. Hence, Zhao et al. [16] proposed modified
330 design equations (Eqs. (25) – (30)) based on the numerical results to predict the nominal
331 flexural strength of CFS section with web openings controlled by distortional buckling.
332 Similarly, Eqs. (31) – (35) were proposed to predict the flexural capacity of CFS sections with
333 web openings controlled by local buckling according to Zhao et al. [16].

$$M_{nd} = M_{ynet} \quad \text{for } \lambda_d \leq \lambda_{d1} \quad (25)$$

$$M_{nd} = M_{ynet} - \left(\frac{M_{ynet} - M_{d2}}{\lambda_{d2} - \lambda_{d1}} \right) (\lambda_d - \lambda_{d1}) \leq 0.88 \left[1 - 0.2 \left(\frac{M_{crd}}{M_y} \right)^{0.45} \right] \left(\frac{M_{crd}}{M_y} \right)^{0.45} M_y \quad (26)$$

$$\text{for } \lambda_{d1} < \lambda_d \leq \lambda_{d2}$$

$$M_{nd} = 0.88 \left[1 - 0.2 \left(\frac{M_{crd}}{M_y} \right)^{0.45} \right] \left(\frac{M_{crd}}{M_y} \right)^{0.45} M_y \quad \text{for } \lambda_d > \lambda_{d2} \quad (27)$$

$$\lambda_{d1} = 0.538 \left(\frac{M_{ynet}}{M_y} \right)^3 \quad (28)$$

$$\lambda_{d2} = 0.538 \left[1.7 \left(\frac{M_y}{M_{ynet}} \right)^{2.7} - 0.7 \right] \quad (29)$$

$$M_{d2} = 0.88 \left(1 - 0.2 \left(\frac{1}{\lambda_{d2}} \right)^{0.9} \right) \left(\frac{1}{\lambda_{d2}} \right)^{0.9} M_y \quad (30)$$

$$M_{ni} = M_{ynet} \quad \text{for } \lambda_l \leq \lambda_a \quad (31)$$

$$M_{nl} = \alpha \left[1 - 0.15 \left(\frac{M_{crl}}{M_{ne}} \right)^{0.4\beta} \right] \left(\frac{M_{crl}}{M_{ne}} \right)^{0.4\beta} M_{ne} \leq M_{ynet} \quad \text{for } \lambda_l > \lambda_a \quad (32)$$

$$\alpha = \left(\frac{M_{ynet}}{M_y} \right)^{19.4 \left(\frac{M_{ynet}}{M_y} \right) - 14.8} \quad (33)$$

$$\beta = \left(\frac{M_{ynet}}{M_y} \right)^{2.1} \quad (34)$$

$$\lambda_a = \text{Solution of the equation } \frac{\alpha \left(1 - \frac{0.15}{\lambda_a^{0.8\beta}} \right)}{\lambda_a^{0.8\beta}} = \frac{M_{ynet}}{M_y} \quad (35)$$

334 Where, M_{nd} – section moment capacity for distortional buckling; M_{ynet} - member yield moment
 335 of net cross-section; M_{crd} - critical elastic distortional buckling moment (including the effect of
 336 web openings; M_y - member yield moment; λ_{d1} , λ_d and λ_{d2} - non-dimensional slenderness
 337 values

338 However, suitability of existing design equations to calculate the section moment capacity of
339 SupaCee sections with web openings was not taken into consideration in the literature. Hence,
340 it is necessary to check the reliability of existing equations to predict the flexural strengths of
341 SupaCee sections with web openings.

342 **6 Design approach for SupaCee sections with web openings**

343 Extensive numerical study was carried out herein to examine the flexural performance of
344 SupaCee sections with web openings. Since the lateral restraints were used in the compression
345 flange of the SupaCee beam for whole section, failure of the section was prominently local
346 buckling. Hence, this section reviews the validity of existing design equation to predict the
347 flexural capacity of SupaCee section without web openings considering the condition of local
348 buckling and introduce new design provisions to calculate the ultimate section moment capacity
349 of SupaCee sections with web openings.

350 Pham and Hancock [3] stated that existing design equations (Eqn. (1) – (3)) were applicable to
351 predict the flexural capacity of SupaCee sections at local buckling as they compared the
352 experiment results with existing equations. Moreover, the researchers [3] investigated the
353 flexural behaviour of SupaCee section with three different cases by changing the limiting
354 moments. Limiting moments of those three cases were yield (M_y), inelastic (M_{ny}), and plastic
355 (M_p) moments, which were defined as Case A, Case B, and Case C respectively in their study.
356 Also, Pham and Hancock [3] proposed Case D with inelastic moment (M_{ny}). However, Case C
357 (using M_p instead of M_{ne}) predicted well the local buckling failure of SupaCee sections. Hence,
358 FE results were compared with proposed DSM-based equation based on Case C. For the
359 comparison of FE results with prediction of Pham and Hancock [3] study, Thin-Wall 2.0 [53],
360 finite strip analysis software was employed to determine the second moment area (I_x) and
361 critical elastic buckling moment (M_{crit}) of those sections. Signature curve and buckling modes
362 of SupaCee section is shown in Fig.19. The comparison of FE results with DSM equation
363 displayed good agreement with the mean value of 1.00 and COV value of 0.08. Fig.20
364 demonstrates the comparison of FE results with existing design equation and experimental
365 results of Pham and Hancock [3] study.

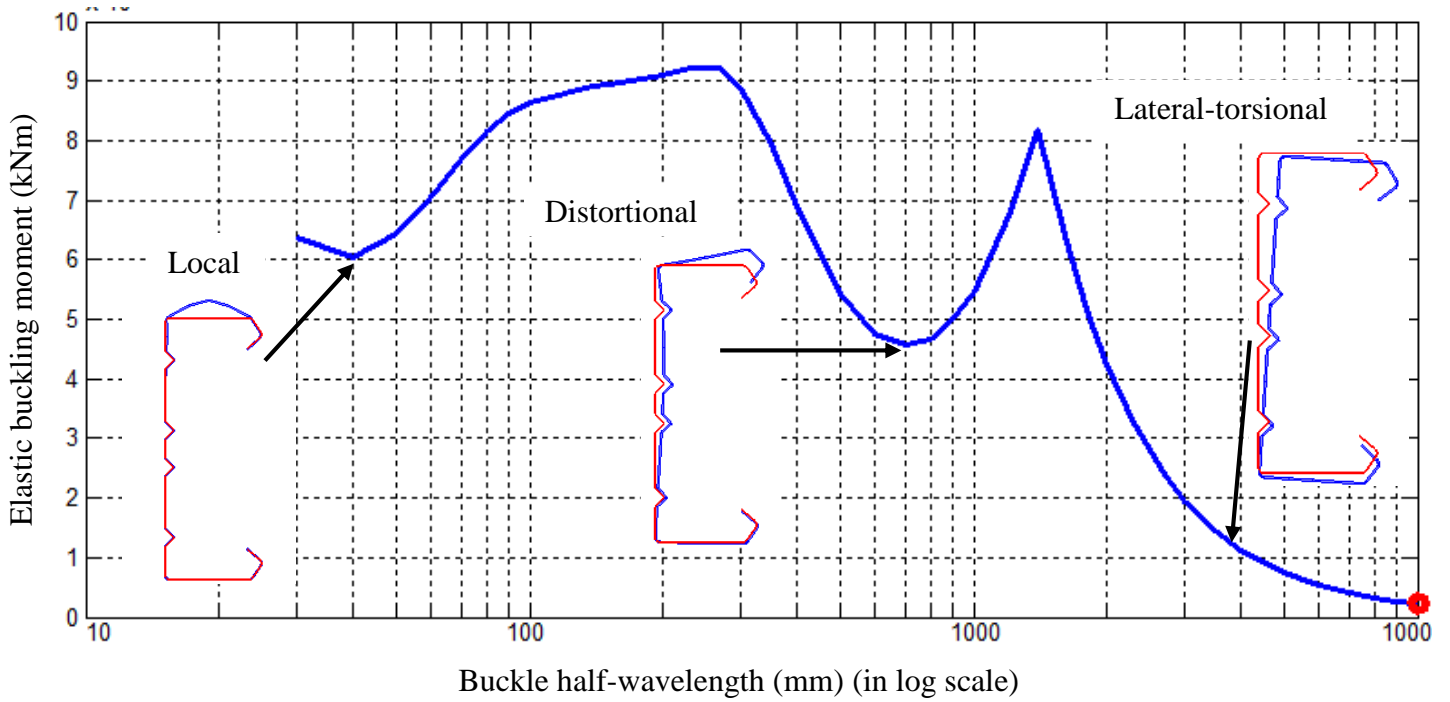


Fig.19: Signature curve and buckle modes of SupaCee section

366

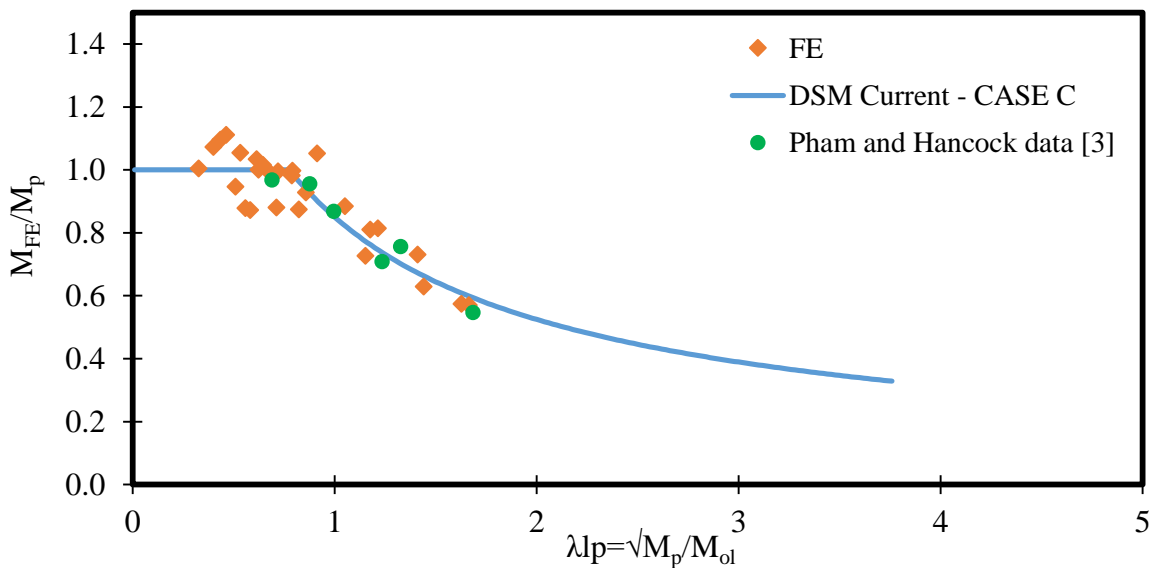


Fig.20: FE results comparison with DSM equation [3]

367

368 Based on the FE results comparison with current DSM equation, it can be concluded that
 369 existing design equation is applicable to predict the section moment capacity of SupaCee
 370 sections without web openings under local buckling condition. However, web opening reduces
 371 flexural capacity of SupaCee section, which should be investigated further and predicted using
 372 design equations.

373 Moen and Schafer [15] and Zhao et al. [16] proposed design equations to predict the flexural
 374 capacity of CFS sections with web openings. The researchers modified the DSM equations to

375 account the reduction causes due to the openings. Since the method was more complex [21], a
 376 simple approach was developed by proposing reduction factors (q_s). Hence, reduction factor
 377 design equations (Eqs. (35) – (37)) were proposed herein considering the key parameters such
 378 as web opening ratio (d_{wh}/d_1) and hole spacing (s) based on the parametric results. Therefore,
 379 ultimate bending capacity of SupaCee sections with openings can be predicted by applying the
 380 proposed reduction factors to their corresponding bending capacity of solid sections, the
 381 bending capacity of solid sections can be determined using DSM equations. Besides, the
 382 comparison of proposed reduction factor equations with numerical results matched well with
 383 the mean value of 1.00 and COV value of 0.11. Fig.21 exhibits the good agreement of proposed
 384 equation with FE results. Moreover, reliability analysis was conducted for the proposed
 385 Eqs.36&37. From the reliability analysis, reduction factor (ϕ_b) of 0.87 is recommended to apply
 386 with the proposed equations.

$$M_{Opening} = M_{solid} \times q_s \quad (35)$$

$$q_s = 0.76 - \left(\frac{d_{wh}}{d_1}\right)^{0.31} + \left(\frac{s}{d_1}\right)^{-0.13} \quad for 0 < \frac{d_{wh}}{d_1} \leq 0.6 \quad (36)$$

$$q_s = 0.75 - \left(\frac{d_{wh}}{d_1}\right)^{0.43} + \left(\frac{s}{d_1}\right)^{-0.32} \quad for 0.6 < \frac{d_{wh}}{d_1} \leq 0.8 \quad (37)$$

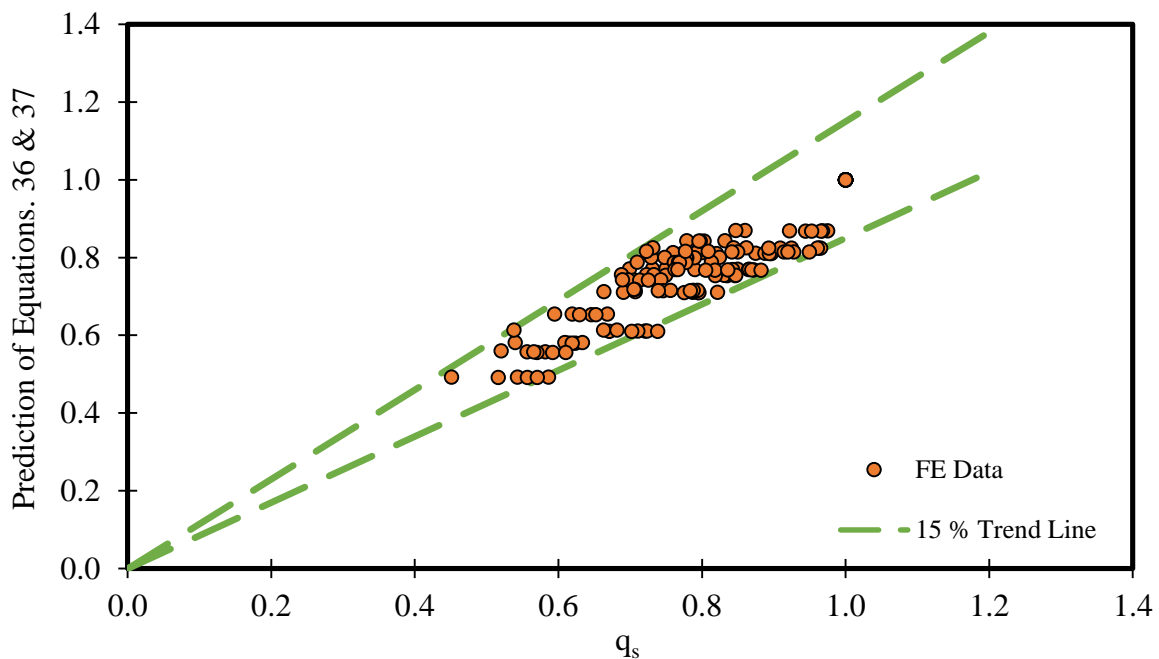
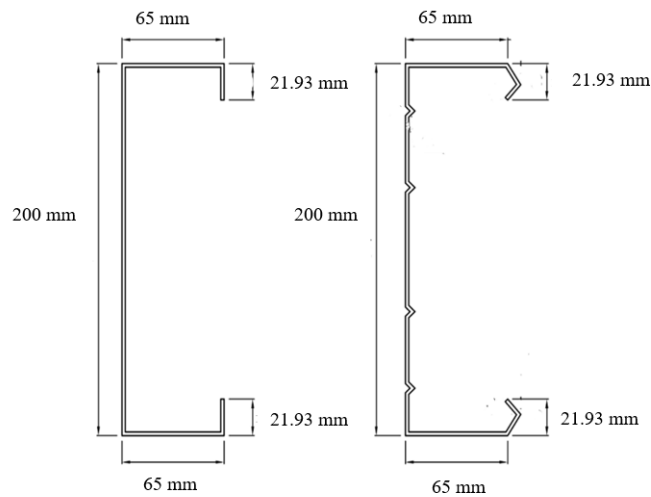


Fig.21: Comparison of proposed reduction factor equation with numerical

388 **7 Comparison of results with LCB sections**

389 This section reviews the applicability of SupaCee sections in the industry, by comparing the
 390 flexural performance of SupaCee sections with similar LCB sections. Therefore, LCB sections
 391 were modelled with the similar dimensions of SupaCee section and numerical analysis was
 392 conducted under similar terms. Fig.22 shows the considered dimensions for this comparative
 393 study. Altogether, 27 models were created incorporating the key parameters such as thickness
 394 (1 mm, 2 mm and 2.5 mm), yield strength (300 MPa, 450 MPa and 600 MPa) and sections;
 395 depth x width (150×50, 200×65 and 250×75). Results for LCB were obtained and compared
 396 with plain SupaCee sections.



397 Fig.22: Comparison of dimensions of LCB and SupaCee section

398 Table.6 presents the flexural capacity comparison between SupaCee and LCB sections. Results
 399 clearly indicated better flexural performance of SupaCee sections; similar statement was
 400 reported earlier by Pham and Hancock [3] based on their experimental results. Moreover,
 401 flexural capacity enhancement of SupaCee section compared to LCB was recorded maximum
 402 of 89.79% and the least was 12.46%. Hence, the application of SupaCee sections in the industry
 403 should be considered as a potential initiative for mass production.

404 Table.6: Flexural capacity comparison of SupaCee sections with Similar LCB

Section depth (mm)	t (mm)	f _y (MPa)	Section moment capacity (kNm)		Section moment capacity increment (%)
			LCB	SupaCee	
150	1	300	2.47	4.12	66.80
150	2	300	6.3	9.05	43.65

150	2.5	300	7.9	10.01	26.71
150	1	450	3.65	5.89	61.37
150	2	450	10.11	13.05	29.08
150	2.5	450	12.8	16.04	25.31
150	1	600	4.6	7.23	57.17
150	2	600	13.42	17.07	27.20
150	2.5	600	17.28	22.15	28.18
200	1	300	3.38	6.04	78.70
200	2	300	9.55	12.98	35.92
200	2.5	300	12.31	17.05	38.51
200	1	450	4.8	9.11	89.79
200	2	450	15.05	21.89	45.45
200	2.5	450	19.05	27.05	41.99
200	1	600	5.58	9.54	70.97
200	2	600	18.59	29.02	56.11
200	2.5	600	23.35	35.89	53.70
250	1	300	5.08	9.55	87.99
250	2	300	16.94	19.05	12.46
250	2.5	300	21.9	26.08	19.09
250	1	450	6.76	11.11	64.35
250	2	450	24.85	28.85	16.10
250	2.5	450	32.27	38.4	19.00
250	1	600	8.35	13.44	60.96
250	2	600	30.27	38.2	26.20
250	2.5	600	40.86	54.02	32.21

405 In addition, flexural performances of Plain LCB was compared to the SupaCee sections with
406 web openings to check the possibilities of replacement of LCB by SupaCee beam with
407 additional advantage of web openings for service integration. Table.7 reports the ultimate
408 flexural capacity comparison of LCB with SupaCee beam with web opening (web opening ratio
409 of 0.4 and 0.6). Results from numerical models exhibited the possibilities for replacing LCB
410 with SupaCee section with web openings ($d_{wh}/d_1 = 0.4$ and 0.6). For all sections, the
411 observations were positive, as the section moment capacity of SupaCee section for both web
412 opening ratios was better than the LCB. Considering the overall results and based on the
413 situations, SupaCee sections with web openings (up to minimum web opening ratio of 0.6) can
414 be a practicable option to replace the LCB. Fig.23 demonstrates the replacement options of
415 SupaCee sections with openings for LCB in terms of flexural capacity comparisons. It indicates
416 that replacement options for section 150 and section 200. Similarly, Fig.24 compares the
417 flexural capacities of section 250 for checking replacement opportunities of SupaCee sections
418 with LCB for different yield strength. For section 250, LCB can be replaced by SupaCee section

419 with web opening ratio of up to 0.8. Hence, based on the flexural capacity comparison SupaCee
 420 section can be utilised in the industry to replace conventional CFS sections with an additional
 421 advantage of web opening.

422 Table.7: Comparison of section moment capacities of LCB with Supacee section with
 423 openings

Section depth (mm)	t (mm)	f _y (MPa)	Section moment capacity (kNm)			Comparison with LCB section (%) ($M_{\text{SupaCee with web opening}} - M_{\text{LCB}} / M_{\text{LCB}} * 100$)	
			LCB	d _{wh} /d ₁ = 0.4	d _{wh} /d ₁ = 0.6	d _{wh} /d ₁ = 0.4	d _{wh} /d ₁ = 0.6
150	1	300	2.47	2.95	2.83	19.43	14.57
150	2	300	6.3	7	6.78	11.11	7.62
150	2.5	300	7.9	8.69	8.36	10.00	5.82
150	1	450	3.65	4.48	4.26	22.74	16.71
150	2	450	10.11	11.41	10.84	12.86	7.22
150	2.5	450	12.8	14.38	13.57	12.34	6.02
150	1	600	4.6	5.73	5.3	24.57	15.22
150	2	600	13.42	15.15	14.46	12.89	7.75
150	2.5	600	17.28	19.79	18.13	14.53	4.92
200	1	300	3.38	4.14	4.05	22.49	19.82
200	2	300	9.55	10.8	10.56	13.09	10.58
200	2.5	300	12.31	13.69	12.98	11.21	5.44
200	1	450	4.8	5.88	5.77	22.50	20.21
200	2	450	15.05	17.05	16.8	13.29	11.63
200	2.5	450	19.05	21.57	21.03	13.23	10.39
200	1	600	5.58	6.93	5.89	24.19	5.56
200	2	600	18.59	21.25	20.6	14.31	10.81
200	2.5	600	23.35	28.57	27.58	22.36	18.12
250	1	300	5.08	7.01	6.9	37.99	35.83
250	2	300	16.94	18.57	18.09	9.62	6.79
250	2.5	300	21.9	24.63	23.85	12.47	8.90
250	1	450	6.76	9.55	8.98	41.27	32.84
250	2	450	24.85	27.92	26.77	12.35	7.73
250	2.5	450	32.27	37.08	35.31	14.91	9.42
250	1	600	8.35	11.39	10.44	36.41	25.03
250	2	600	30.27	35.22	32.46	16.35	7.23
250	2.5	600	40.86	51.46	45.46	25.94	11.26

424

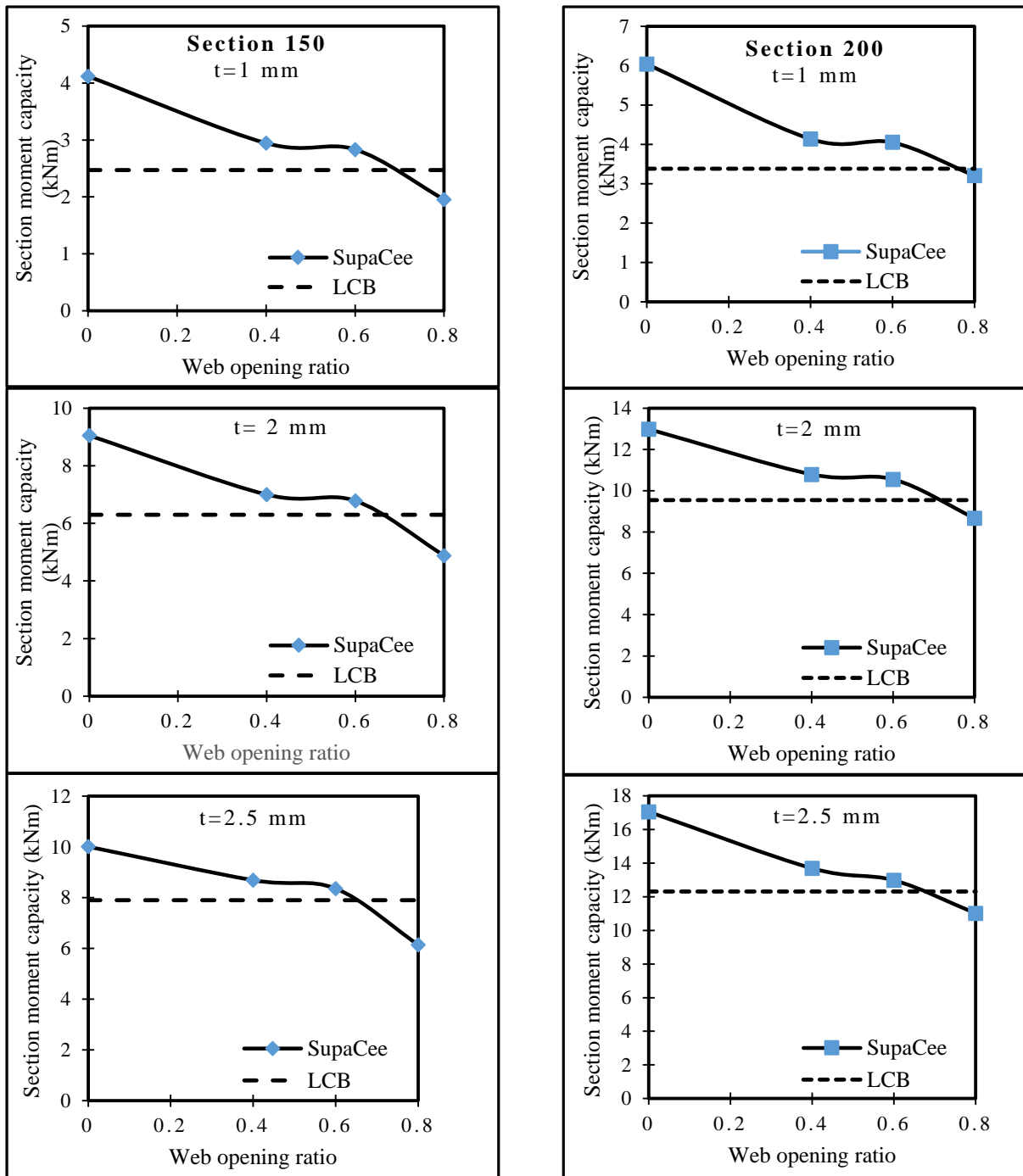


Fig.23: Flexural capacity comparison between LCB and SupaCee section with holes ($f_y = 300$ MPa) for different thicknesses

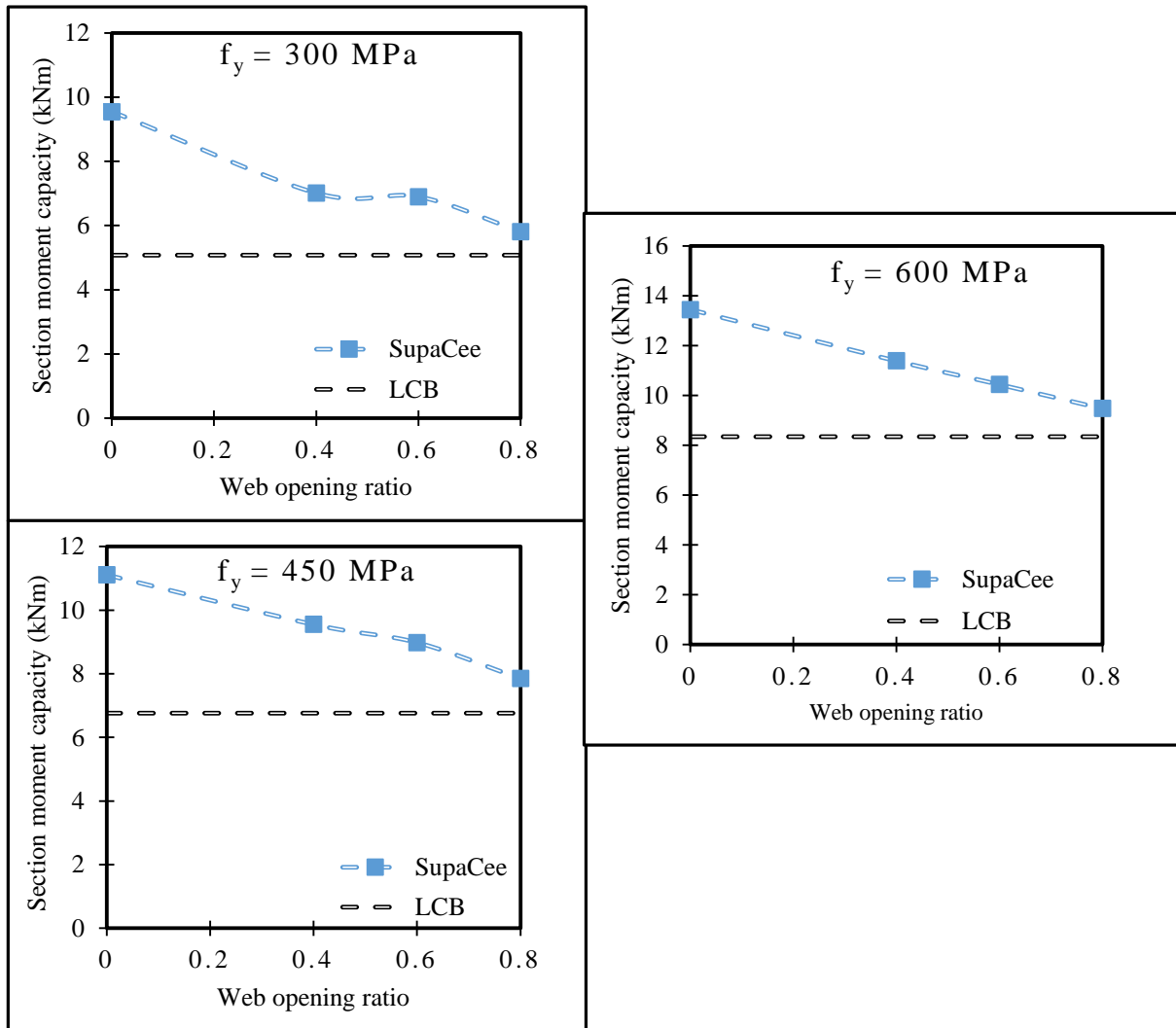


Fig.24: Flexural capacity comparison between LCB and SupaCee section with holes for section 250 (thickness = 1 mm)

426

427 8 Conclusion

428 This paper has reported a detailed investigation on flexural performance of SupaCee sections
 429 with web openings. Numerical analysis was initiated with validation followed by the
 430 implementation of parametric plan covering wide range of key parameters. Results were
 431 analysed while comparisons and recommendations were stated for considered key parameters.
 432 Since hole spacing was not considered in previous studies as a key parameter to format an
 433 equation to predict the ultimate bending moment, existing design equations are found
 434 inappropriate to compare the FE results. Hence, based on the numerical results new design
 435 provisions were proposed to predict the ultimate flexural capacities of SupaCee sections with
 436 web openings under predominantly local buckling failure scenario. Further, LCB sections were
 437 modelled to similar to SupaCee sections and ultimate flexural capacity of both LCB and

438 SupaCee sections with and without web openings were compared. Comparison displayed about
439 12.46 – 89.79 % enhancement in flexural capacity in plain SupaCee sections. Besides, better
440 flexural capacities were observed in SupaCee section with web openings (beyond web opening
441 ratio of 0.6) compared to LCB. Hence, this paper recommends the practical application of
442 SupaCee sections as a replacement of conventional CFS sections including LCB with an
443 additional advantage of having web openings for service integrations considering the
444 comparison of flexural performance. Overall, this study concludes that proposed design
445 equations do accurately predict the flexural capacity of SupaCee sections with web openings
446 and recommends design considerations and applicability of SupaCee section with web
447 openings in the industry. However, since the study was conducted using numerical approaches
448 purely, the proposed equations could be verified with experimental results for more accuracy.

449 **9 Acknowledgements**

450 The authors would like to acknowledge the supports provided by the Northumbria University,
451 European research council and The Home Engineers.

452 **References**

- 453 [1] P. Gatheeshgar, K. Poologanathan, S. Gunalan, K. D. Tsavdaridis, B. Nagaratnam, and
454 E. Iacovidou, “Optimised cold-formed steel beams in modular building applications,” *J.*
455 *Build. Eng.*, vol. 32, p. 101607, 2020.
- 456 [2] P. C. Hung, B. L. A., and G. J. Hancock, “Experimental Study of Longitudinally
457 Stiffened Web Channels Subjected to Combined Bending and Shear,” *J. Struct. Eng.*,
458 vol. 141, no. 11, p. 4015018, Nov. 2015.
- 459 [3] P. C. Hung and G. J. Hancock, “Experimental Investigation and Direct Strength Design
460 of High-Strength, Complex C-Sections in Pure Bending,” *J. Struct. Eng.*, vol. 139, no.
461 11, pp. 1842–1852, Nov. 2013.
- 462 [4] B. Chen, K. Roy, A. Uzzaman, and J. B. P. Lim, “Moment capacity of cold-formed
463 channel beams with edge-stiffened web holes, un-stiffened web holes and plain webs,”
464 *Thin-Walled Struct.*, vol. 157, p. 107070, 2020.
- 465 [5] “Service holes for plumbing and electrical - Spantec.” [Online]. Available:
466 [https://spantec.com.au/products/boxspan-upper-floor-frames/upper-floor-](https://spantec.com.au/products/boxspan-upper-floor-frames/upper-floor-gallery/olympus-digital-camera-4/)
467 [gallery/olympus-digital-camera-4/](https://spantec.com.au/products/boxspan-upper-floor-frames/upper-floor-gallery/olympus-digital-camera-4/). [Accessed: 04-Jan-2022].

- 468 [6] “Service integration - SteelConstruction.info.” [Online]. Available:
469 https://www.steelconstruction.info/Service_integration. [Accessed: 04-Jan-2022].
- 470 [7] Y. Cheng and S. B. W., “Distortional Buckling Tests on Cold-Formed Steel Beams,” *J.*
471 *Struct. Eng.*, vol. 132, no. 4, pp. 515–528, Apr. 2006.
- 472 [8] C. Yu and B. W. Schafer, “Simulation of cold-formed steel beams in local and
473 distortional buckling with applications to the direct strength method,” *J. Constr. Steel*
474 *Res.*, vol. 63, no. 5, pp. 581–590, 2007.
- 475 [9] C. Yu and W. Yan, “Effective Width Method for determining distortional buckling
476 strength of cold-formed steel flexural C and Z sections,” *Thin-Walled Struct.*, vol. 49,
477 no. 2, pp. 233–238, 2011.
- 478 [10] N. Dolamune Kankanamge and M. Mahendran, “Behaviour and design of cold-formed
479 steel beams subject to lateral–torsional buckling,” *Thin-Walled Struct.*, vol. 51, pp. 25–
480 38, 2012.
- 481 [11] M. Anbarasu, “Local-distortional buckling interaction on cold-formed steel lipped
482 channel beams,” *Thin-Walled Struct.*, vol. 98, pp. 351–359, 2016.
- 483 [12] M. R. Haidarali and D. A. Nethercot, “Finite element modelling of cold-formed steel
484 beams under local buckling or combined local/distortional buckling,” *Thin-Walled*
485 *Struct.*, vol. 49, no. 12, pp. 1554–1562, 2011.
- 486 [13] L. Wang and B. Young, “Design of cold-formed steel channels with stiffened webs
487 subjected to bending,” *Thin-Walled Struct.*, vol. 85, pp. 81–92, 2014.
- 488 [14] P. Gatheeshgar, S. Parker, K. Askew, K. Poologanathan, S. Navaratnam, A. McIntosh,
489 and D. Widdowfield Small, “Flexural behaviour and design of modular construction
490 optimised beams,” *Structures*, vol. 32, pp. 1048–1068, 2021.
- 491 [15] C. D. Moen and B. W. Schafer, “Elastic buckling of cold-formed steel columns and
492 beams with holes,” *Eng. Struct.*, vol. 31, no. 12, pp. 2812–2824, 2009.
- 493 [16] J. Zhao, K. Sun, C. Yu, and J. Wang, “Tests and direct strength design on cold-formed
494 steel channel beams with web holes,” *Eng. Struct.*, vol. 184, pp. 434–446, 2019.
- 495 [17] N. Yu, B. Kim, W. Yuan, L. Li, and F. Yu, “An analytical solution of distortional

- 496 buckling resistance of cold-formed steel channel-section beams with web openings,”
497 *Thin-Walled Struct.*, vol. 135, pp. 446–452, 2019.
- 498 [18] G. J. Hancock, “Design for distortional buckling of flexural members,” *Thin-Walled*
499 *Struct.*, vol. 27, no. 1, pp. 3–12, 1997.
- 500 [19] T. K. Daniel and D. Cedric, “Vierendeel Bending Study of Perforated Steel Beams with
501 Various Novel Web Opening Shapes through Nonlinear Finite-Element Analyses,” *J.*
502 *Struct. Eng.*, vol. 138, no. 10, pp. 1214–1230, Oct. 2012.
- 503 [20] N. Degtyareva, P. Gatheeshgar, K. Poologanathan, S. Gunalan, K. D. Tsavdaridis, and
504 S. Napper, “New distortional buckling design rules for slotted perforated cold-formed
505 steel beams,” *J. Constr. Steel Res.*, vol. 168, p. 106006, 2020.
- 506 [21] N. Degtyareva, P. Gatheeshgar, K. Poologanathan, S. Gunalan, I. Shyha, and A.
507 McIntosh, “Local buckling strength and design of cold-formed steel beams with slotted
508 perforations,” *Thin-Walled Struct.*, vol. 156, p. 106951, 2020.
- 509 [22] K. Poologanathan and M. Mahendran, “New Design Rules for the Shear Strength of
510 LiteSteel Beams with Web Openings,” *J. Struct. Eng.*, vol. 139, no. 5, pp. 640–656, May
511 2013.
- 512 [23] K. S. Wanniarachchi, M. Mahendran, and P. Keerthan, “Shear behaviour and design of
513 Lipped Channel Beams with non-circular web openings,” *Thin-Walled Struct.*, vol. 119,
514 pp. 83–102, 2017.
- 515 [24] P. Keerthan and M. Mahendran, “Experimental studies of the shear behaviour and
516 strength of lipped channel beams with web openings,” *Thin-Walled Struct.*, vol. 73, pp.
517 131–144, 2013.
- 518 [25] P. Keerthan and M. Mahendran, “Improved shear design rules for lipped channel beams
519 with web openings,” *J. Constr. Steel Res.*, vol. 97, pp. 127–142, 2014.
- 520 [26] P. Keerthan and M. Mahendran, “Shear Behaviour and Strength of LiteSteel Beams with
521 Web Openings,” *Adv. Struct. Eng.*, vol. 15, no. 2, pp. 171–184, Feb. 2012.
- 522 [27] D. L. Chandramohan, E. Kanthasamy, P. Gatheeshgar, K. Poologanathan, M. F. M.
523 Ishqy, T. Suntharalingam, and T. Kajaharan, “Shear behaviour and design of doubly
524 symmetric hollow flange beam with web openings,” *J. Constr. Steel Res.*, vol. 185, p.

- 525 106836, 2021.
- 526 [28] H. Sun, B. Cao, Z. Chen, and Y. Du, "Shear behaviour of reinforced straw-bale plaster
527 sheathed cold-formed steel-framed shear walls," *Biosyst. Eng.*, vol. 221, pp. 54–68,
528 2022.
- 529 [29] N. Degtyareva, P. Gatheeshgar, K. Poologanathan, S. Gunalan, M. Lawson, and P.
530 Sunday, "Combined bending and shear behaviour of slotted perforated steel channels:
531 Numerical studies," *J. Constr. Steel Res.*, vol. 161, pp. 369–384, 2019.
- 532 [30] M. F. M. Ishqy, S. Wanniarachchi, and K. Poologanathan, "Shear behaviour of screw
533 fastened rectangular hollow flange beams with web openings," *J. Constr. Steel Res.*, vol.
534 189, p. 107019, 2022.
- 535 [31] K. Thirunavukkarasu, E. Kanthasamy, K. Poologanathan, K. D. Tsavdaridis, P.
536 Gatheeshgar, S. Hareindirasarma, and A. McIntosh, "Shear performance of SupaCee
537 sections with openings: Numerical studies," *J. Constr. Steel Res.*, vol. 190, p. 107142,
538 2022.
- 539 [32] H. Alsanat, S. Gunalan, P. Gatheeshgar, K. Poologanathan, and A. M. Thabet, "Design
540 of roll-formed aluminium lipped channel sections with web opening subjected to web
541 crippling under end-two-flange load case," *J. Build. Eng.*, vol. 48, p. 103887, 2022.
- 542 [33] A. McIntosh, P. Gatheeshgar, S. Gunalan, E. Kanthasamy, K. Poologanathan, M.
543 Corradi, and C. Higgins, "Unified approach for the web crippling design of cold-formed
544 channels: Carbon steel, stainless steel and aluminium," *J. Build. Eng.*, vol. 51, p. 104134,
545 2022.
- 546 [34] Z. Fang, K. Roy, J. Xu, Y. Dai, B. Paul, and J. B. P. Lim, "A novel machine learning
547 method to investigate the web crippling behaviour of perforated roll-formed aluminium
548 alloy unlipped channels under interior-two flange loading," *J. Build. Eng.*, vol. 51, p.
549 104261, 2022.
- 550 [35] P. Keerthan, M. Mahendran, and E. Steau, "Experimental study of web crippling
551 behaviour of hollow flange channel beams under two flange load cases," *Thin-Walled*
552 *Struct.*, vol. 85, pp. 207–219, 2014.
- 553 [36] K. Elilarasi, S. Kasthuri, and B. Janarthanan, "Effect of circular openings on web

- 554 crippling of unlippped channel sections under end-two-flange load case,” *Adv. Steel*
555 *Constr.*, vol. 16, no. 4, pp. 310–320, 2020.
- 556 [37] K. Thirunavukkarasu, E. Kanthasamy, P. Gatheeshgar, K. Poologanathan, S. Das, S.
557 Todhunter, and T. Suntharalingam, “Web crippling design of modular construction
558 optimised beams under ETF loading,” *J. Build. Eng.*, vol. 43, p. 103072, 2021.
- 559 [38] S. Hareindirasarma, K. Elilarasi, and B. Janarthanan, “Effect of circular holes on the web
560 crippling capacity of cold-formed LiteSteel beams under Interior-Two-Flange load
561 case,” *Thin-Walled Struct.*, vol. 166, p. 108135, 2021.
- 562 [39] K. Elilarasi and B. Janarthanan, “Effect of web holes on the web crippling capacity of
563 cold-formed LiteSteel beams under End-Two-Flange load case,” *Structures*, vol. 25, pp.
564 411–425, 2020.
- 565 [40] P. Gatheeshgar, H. Alsanat, K. Poologanathan, S. Gunalan, N. Degtyareva, S.
566 Wanniarachchi, and I. Fareed, “Web crippling of slotted perforated Cold-Formed Steel
567 channels under EOF load case: Simulation and design,” *J. Build. Eng.*, vol. 44, p.
568 103306, 2021.
- 569 [41] P. Gatheeshgar, H. Alsanat, K. Poologanathan, S. Gunalan, N. Degtyareva, and I.
570 Hajirasouliha, “Web crippling behaviour of slotted perforated cold-formed steel
571 channels: IOF load case,” *J. Constr. Steel Res.*, vol. 188, p. 106974, 2022.
- 572 [42] K. D. Tsavdaridis and C. D’Mello, “Web buckling study of the behaviour and strength
573 of perforated steel beams with different novel web opening shapes,” *J. Constr. Steel*
574 *Res.*, vol. 67, no. 10, pp. 1605–1620, 2011.
- 575 [43] K. D. Tsavdaridis and G. Galiatsatos, “Assessment of cellular beams with transverse
576 stiffeners and closely spaced web openings,” *Thin-Walled Struct.*, vol. 94, pp. 636–650,
577 2015.
- 578 [44] Dassault Systems Simulia Corp, “Abaqus/CAE 2017 User’s Guide,” *Abaqus/CAE*
579 *Standard 2017*. 2017.
- 580 [45] C. H. Pham and G. J. Hancock, “Numerical simulation of high strength cold-formed
581 supacee® sections in combined bending and shear,” *Res. Rep. - Univ. Sydney, Dep. Civ.*
582 *Eng.*, no. 913, 2010.

- 583 [46] Thirunavukkarasu K, Kanthasamy E, Gatheeshgar P, Poologanathan K, Rajanayagam
584 H, Suntharalingam T, Dissanayake M. Sustainable Performance of a Modular Building
585 System Made of Built-Up Cold-Formed Steel Beams. *Buildings*. 2021; 11(10):460.
- 586 [47] N. Perera and M. Mahendran, “Finite element analysis and design for section moment
587 capacities of hollow flange steel plate girders,” *Thin-Walled Struct.*, vol. 135, pp. 356–
588 375, 2019.
- 589 [48] E. Kanthasamy, K. Thirunavukkarasu, K. Poologanathan, P. Gatheeshgar, S. Todhunter,
590 T. Suntharalingam, and M. Fareedh Muhammadh Ishqy, “Shear behaviour of doubly
591 symmetric rectangular hollow flange beam with circular edge-stiffened openings,” *Eng.*
592 *Struct.*, vol. 250, p. 113366, 2022.
- 593 [49] B. W. Schafer, Z. Li, and C. D. Moen, “Computational modeling of cold-formed steel,”
594 *Thin-Walled Struct.*, vol. 48, no. 10, pp. 752–762, 2010.
- 595 [50] American Iron and Steel Institute (AISI), Specifications for the cold-formed steel
596 structural members, cold-formed steel design manual, AISI S100, Washington DC,
597 USA; 2016.
- 598 [51] Australia/New Zealand Standard AS/NZS 4600 Cold-Formed Steel Structures,
599 Standards Australia/Standards New Zealand (SA), Sydney, Australia, 2018.
- 600 [52] S. Yared and S. B. W., “Inelastic Bending Capacity of Cold-Formed Steel Members,”
601 *J. Struct. Eng.*, vol. 138, no. 4, pp. 468–480, Apr. 2012.
- 602 [53] V.V. Nguyen, G.J. Hancock, C.H. Pham, Application of the THIN-WALL-2 V2.0
603 Program for Analysis of Thin-Walled Sections Under Localised Loading, Proceedings
604 of the 4th Congr`es International de G´eotechnique - Ouvrages -Structures2018, pp. 78-
605 88.